

AD-A145 969

NOVEL TRANSPORT AND RECOMBINATION PROCESSES IN
SEMICONDUCTORS(U) CAMBRIDGE UNIV (ENGLAND) CAVENDISH
LAB H PEPPER MAR 84 DAJA37-82-C-0181

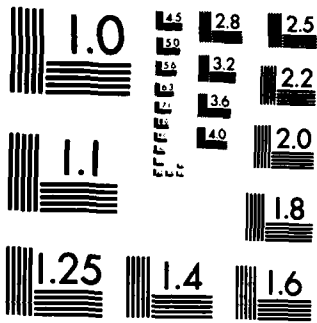
1/1

UNCLASSIFIED

F/G 28/12

NL

END



MICROCOPY RESOLUTION TEST CHART
NATIONAL BUREAU OF STANDARDS-1963-A

AD-A145 969

(1)

4072-EE

NOVEL TRANSPORT AND RECOMBINATION
PROCESSES IN SEMICONDUCTORS

ANNUAL TECHNICAL REPORT

by

M. PEPPER

MARCH 1984

EUROPEAN RESEARCH OFFICE

United States Army

London. England

CONTRACT NUMBER DAJA37-82-C-0181

GR: Cavendish Laboratory
Department of Physics
University of Cambridge
Cambridge
CB3 0HE
U.K.

DTIC
SELECTED
SEP 27 1984
A

DTIC FILE COPY

Approved for Public Release: distribution unlimited

DTIC
UNCLASSIFIED

ABSTRACT

This report describes our work on spin dependent recombination to date and contains copies of preprints and reprints of our work on two dimensional transport.

Our work on spin effects has succeeded in identifying both spin dependent generation and recombination. The obtained structure is described and it is shown that damage produced by avalanche injection of holes gives rise to an SDR signal.

The major feature of our work on the electronic properties of two dimensional systems is the frequency production of fractional quantisation in Si inversion layers and GaAs-AlGaAs heterojunctions. Decreasing the transport length scale reduces the role of disorder and enhances the electron-electron interaction. This work leads to the possibility of observation of a number of effects based on a trade off between localisation and interactions. Other 2D topics discussed are the effects of the electron-electron interaction on transport in high magnetic fields and the role of disorder in altering the rate of electron-electron scattering.



2. INTRODUCTION

We present the abstracts of preprints and reprints of the work supported by this contract. The complete description of this work is in section 5.

3. PUBLICATIONS SUPPORTED BY THIS CONTRACT

1. 'Electron-electron scattering in silicon inversion layers'; R.A. Davies and M. Pepper, J. Phys. C. 16, L353-L360, 1983.
2. 'Non-metallic transport in silicon inversion layers and the Hall effect'; R.A. Davies and M. Pepper, J. Phys.C 16 L361-L367, 1983.
3. 'Two dimensional electron interaction effects in high magnetic fields', R.A. Davies and M. Pepper, J. Phys. C 16, L679-L685, 1983.

4. DEFECT PRODUCED SPIN DEPENDENT RECOMBINATION (SDR) IN Si p-n JUNCTIONS. M. PEPPER AND R. VRANCH

Recombination

The experiments are performed at room temperature on MOS field-effect transistors used as gate-controlled diodes (figure 1). The diode between the p diffusion and the n substrate is operated in small forward bias so that the current is dominated by recombination in the depletion region: the depletion region can be extended by the application of a negative gate voltage to include (radiation induced) interface states at the Si-SiO₂ interface.

Spin-Dependent Recombination (SDR) is observed as an enhancement of the recombination current when a magnetic field B is swept through the resonance condition $g\mu B = h\nu$, where μ is the Bohr magneton and ν is the frequency of a microwave or radiofrequency magnetic field perpendicular to B. The value of g is deduced from this equation as in conventional ESR. A typical signal, from a (100) MOS device irradiated with 30 keV electrons, is shown in figure 2. It is measured as a first derivative of current by lock-in detection at the frequency of modulation of the swept field B. The sign of the

enhancement is opposite to that of a first derivative degradation of current caused by a DPPM absorber in the cavity, which causes a resonant reduction in the pickup of stray microwave electric field by the sample.

In conventional ESR, any unpaired spin contributes to microwave absorption but a large area of interface is required to detect a signal. SDR is only detected when an electron-hole recombination is affected by the spin resonance, but as long as such recombination dominates the conduction process the resonance can be measured in arbitrarily small samples. Hence the results below are particularly significant in that they have been obtained by non-destructive electrical measurements on small, working, devices which have been degraded in similar ways to MOS devices in practical systems.

The size of the enhancement, $I(\text{SDR})/I_{\text{REC}}$ is about 5×10^{-4} . The main error in estimating this quantity is in measuring the fraction of the diode current $I(\text{dc})$ that is the recombination current I_{REC} . Radiation-induced recombination centres increase the fraction $I_{\text{REC}}/I(\text{dc})$ by an order of magnitude, but SDR is only seen in devices with large numbers of defects. This indicates that the pre-irradiation density of centres is not sufficient to observe a spin-dependent effect. The best model to explain the large size of the effect does indeed rely on the interaction between adjacent trapped electrons and holes (D. Kaplan, I. Solomon and N.F. Mott, *J-de Physique Lettres* 39, L-51, 1978). Without such a pair model, one can only account for an enhancement of about 10^{-6} at room temperature since the polarisation of free spins in B is small.

The gist of the model is that trapped electron-hole pairs cannot recombine if the two spins are 'parallel' (strictly, if they are in a triplet symmetric spin state). At resonance, one of the spins is 'flipped' to produce a singlet pair, which can recombine, enhancing the recombination current. Therefore one would expect to see two resonances, corresponding to the electron or the hole. Usually, one broad resonance is seen (figure 2). It is Gaussian in shape, and the linewidth is reduced when the microwave frequency is reduced to 7GHz, with a proportional reduction in B for the resonance. This

inhomogenous line broadening indicates that more than one g-value is in the SDR signal.

The resonance has also been observed at a field of about 15.5 mT (1mT=10 Gauss) and a corresponding radio frequency of 440MHz. The fact that the signal is found to be the same size at this field is a convincing test of the prediction of the trapped pair model of Kaplan et al, that the signal size should be field-independent.

The g-value on (100) devices for B normal to the (100) is $2.0051 \pm .0003$. At present, anisotropy measurements are not as easy as in conventional ESR work, due to the device packaging, but this is good evidence of the surface recombination centres being P_t centres as observed by ESR initially by Nishi, and investigated recently by groups at Sandia, ERADCOM and elsewhere.

SPIN DEPENDENT GENERATION (SDG)

The reverse current in a diode is dominated by the generation of carriers in the depletion region. This is a consequence of the statistics of the capture and emission of electrons and holes by generation-recombination centres. A reverse biased diode shows a spin resonance signal with the same shape and position as the SDR signal, but of opposite sign. This corresponds to an enhancement of the (negative) generation current and will be referred to as SDG. Irradiated devices have enlarged reverse 'leakage' currents because of the increased number of recombination-generation centres, but the current is small (about 1nA) compared to forward currents. However, since the effect of microwave electric field pickup is less significant in reverse bias, the signal to noise ratio is often bigger for the SDG signal, so it is often used in preference to SDR to investigate the spin dependence. SDG signals are also easier to interpret, since the reverse current is dominated by generation, whereas the SDR signal must be considered with allowance for the fraction of $I(dc)$ which is recombination current.

Incident light affects the direct current through the diode by band to band generation of carriers, and can even reverse the sign of the current, but it has no effect on the SDR or SDG signals. This

implies that the number of the free carriers is not important in the spin dependent process.

Small resonances recently detected on either side of the main (111) signal are very similar to the ^{29}Si hyperface structure recently reported in ESR measurements by Brower (Appl. Phys. Lett. 43 (12), 1111, (1983). Electron-Nuclear Double Spin Dependent Resonance experiments have so far not been successful in resolving the hyper-fine structure more clearly.

MNOS Devices

Experiments have been performed on a batch of (111) MNOS devices with a 2 nm oxide layer which have far greater interface recombination than most irradiated MOS devices. They do not suffer from the inhomogeneity of radiation-induced trapped positive oxide charge that can smear out any gate voltage dependencies (for example C-V plots).

The signals vary from sample to sample, and one is shown in figure 3. Two separate resonances are clearly resolved. The data can be fitted to a pair of Gaussian derivatives of width 0.75 mT, centred 0.6 mT apart. The g-values of the MNOS signals are generally much bigger than the MOS p_{h} centres. This could be due to an interaction with an impurity (iron for example) or it could be related to the electron-hole in the triplet state.

The energy diagram for a triplet is shown in figure 4. The position of the singlet level S_0 depends on the exchange interaction between the spins. Note that if the zero-field splitting D is large enough, the transitions described above corresponding to one spin 'flipping' (marked with arrows) of length $h\nu$ will occur at different g-values for the electron and hole. Using the data of figure 3, D can be estimated from the difference in magnetic field between the two resonances, and using a formula for the dipole-dipole interaction between adjacent spins (W. Gordy, 'Theory and Applications of ESR', Wiley, 1980) the separation between the spins is estimated to be 1.4 nm. There are two further interesting properties of systems which are described by a triplet energy level diagram. These will now be described.

The first is that at a magnetic field of about half that of the resonances described above, the applied microwave energy quantum can excite transitions between the upper and lower triplet levels. This 'half-field' or $m_s = 2$, resonance has been observed in an irradiated MOS device (figure 5). The signal was an enhancement at 7 GHz but a degradation at 9.4 GHz. Work is in progress to understand these results in terms of how these transitions affect the recombination statistics. This involves the question of the position of the signal level on the triplet energy diagram in figure 4. The size of the zero-field splitting D, and also the possibility of a further split E between the 1 and -1 levels at zero field, will affect the positions of the microwave induced transitions on the magnetic field axis, and will also affect the transition probability for the normally forbidden $m_s = 2$ transition. D and E should vary with the orientation of B with respect to the crystal axes.

The second property is that even without a microwave field, as B is reduced and 0 level crosses the -1 level, transitions can occur between these levels. This is a 'spin temperature' effect which arises because the Zeeman energy difference between the level is comparable to the dipole-dipole energy between the spins. (Normally, the dipole-dipole interaction simply determines the width of the spin resonance between the well-spaced Zeeman levels). Non-resonant effects of this kind are described below. For a description of triplet recombination in amorphous materials observed by optically detected magnetic resonance, see a review by B.C. Cavenett, (Adv. Phys., 30, (4), 475).

NON-RESONANCE EXPERIMENTS

Sweeping the magnetic field without a microwave field reveals 'resonances' that show up as enhancements of the recombination or generation current (figure 6). These resonances only appear in devices that show conventional resonant SDR signals, and they respond to biasing and light in the same way as the high-field resonances do. Because of the lack of microwave interference, the signal to noise ratio is excellent, but of course no information about g-values can be obtained. There is no analogy with conventional ESR here. The experiment is in effect measuring a magnetoresistance by phase

sensitive detection in a system where the conductivity is dominated by SDR. Similar non-resonant effects have been observed in the luminescence and photoconductivity of amorphous silicon. Explorations which rely on geminate pairs, spin dephasing and spin-dependent hopping have been proposed.

The signals are always symmetric about zero magnetic field and are of similar width to the conventional spin resonances, but have tails either side of the centre that are wider even than a Lorentzian derivative. This implies that the 'level-mixing' begins to be effective at $B \pm 4\text{mT}$, so the resonance is wide. The size of the non-resonant signal is about the same or slightly bigger than the saturated resonance signals (it requires just over one watt of microwave power for the saturation of resonant SDR.) Both SDR and SDG signals can be detected.

Variation of the angle between the magnetic field and the sample can cause structure to appear at the centre of the non-resonant signal (figure 7). As in figure 3, the centre structure results from the addition of two clearly spaced resonances, though here we are seeing the same resonance twice, centred symmetrically at equivalent positive and negative magnetic fields. In figure 6 the resonance was centred at zero field, so it appears only as a single derivative.

For (111) devices, the structure is not seen for $B \parallel [111]$, and centre structure of peak to peak width 0.4mT appears with $B \parallel [111]$. The structure probably arises between B and $[111]$, which modifies the point at which the 0 and - levels cross to give the non-resonant signal. The structure is isotropic about the $[111]$ direction, which is responsible for the SDR effect. The centre structure on (100) devices shows a more complicated angular dependence, but it can be explained qualitatively by considering the sum of the the $[111]$ axially symmetric dependencies just described, orientated along the $[111]$ and $[\bar{1}\bar{1}\bar{1}]$ directions at the (100) interface.

MODULATION FREQUENCY DEPENDENCE

The non-resonant SDR signal was used to investigate the variation of the size of the effect with the frequency

of the modulation of the swept magnetic field. The result is shown in figure 8. It is very similar to the result of Lenahan and Schubert on the frequency response of the spin-dependent trapping at a silicon grain boundary. The normalised signal varies as $(\omega^2\tau^2+1)^{-1}$ where ω is 2π times the modulation frequency, and τ is a carrier emission time. From the data of figure 8, a value of $\tau = 1.0 \times 10^{-4}$ seconds is obtained.

ELECTRICAL INJECTION OF HOLES

High frequency avalanche injection of holes into the oxide of MOS capacitors has been used to investigate the radiation hardness of gate oxides. This technique cannot be used on MOS devices due to edge breakdown and other limitations (see Nicollian and Brews, 'MOS Physics and Technology', Wiley, 1982). It is possible to inject holes in a MOSFET by using the avalanche of the p-n diode between the diffusion and substrate. This is related to the additional problems caused by hot carrier trapping and injection that can degrade MOS devices even in non-radiation environments.

For this work, n-channel gate-controlled diodes were used, and the n-diffusion to p-substrate diode was avalanched while a gate voltage of -10v was applied to pull holes into the oxide. Severe degradation of the Si-SiO₂ interface was produced in the region of the diffusions, and large SDR and SDG signals were observed after the avalanche.

This demonstrates the potential usefulness of the technique for investigating the nature of the defects produced in real MOS devices by a variety of degradation mechanisms that the device will encounter in its working life. ESR will not be able to provide such information, as it can only be used on large area wafers. SDR can give information about defects introduced in device fabrication and operation, by non destructive measurements that can be performed in-situ.

FIGURE CAPTIONS

- Figure 1 MOS gate-controlled diode.
- Figure 2 A typical SDR signal with microwaves at 9.4 GHz (the DPPH g-marker is also shown).
- Figure 3 An example of an SDG signal from an unirradiated MNOS device.
- Figure 4 Energy Diagram for a triplet (T_1 , T_0 , T_{-1}) and singlet (S_0) in a magnetic field. The spin wave-functions (\uparrow up and \downarrow down) for the pair are also shown.
- Figure 5 The normal SDR signal at 0,34T, with the broad half-field resonance at 0.17T (microwaves at 9.4 GHz).
- Figure 6 A typical non-resonant SDR signal.
- Figure 7 Non-resonant SDR signal for $B \parallel [111]$, showing centre structure symmetric about zero field.
- Figure 8 Normalised SDR signal size plotted against modulation frequency.

5. APPENDIX OF REPRINTS OF WORK SUPPORTED BY THIS CONTRACT

FIG. 1

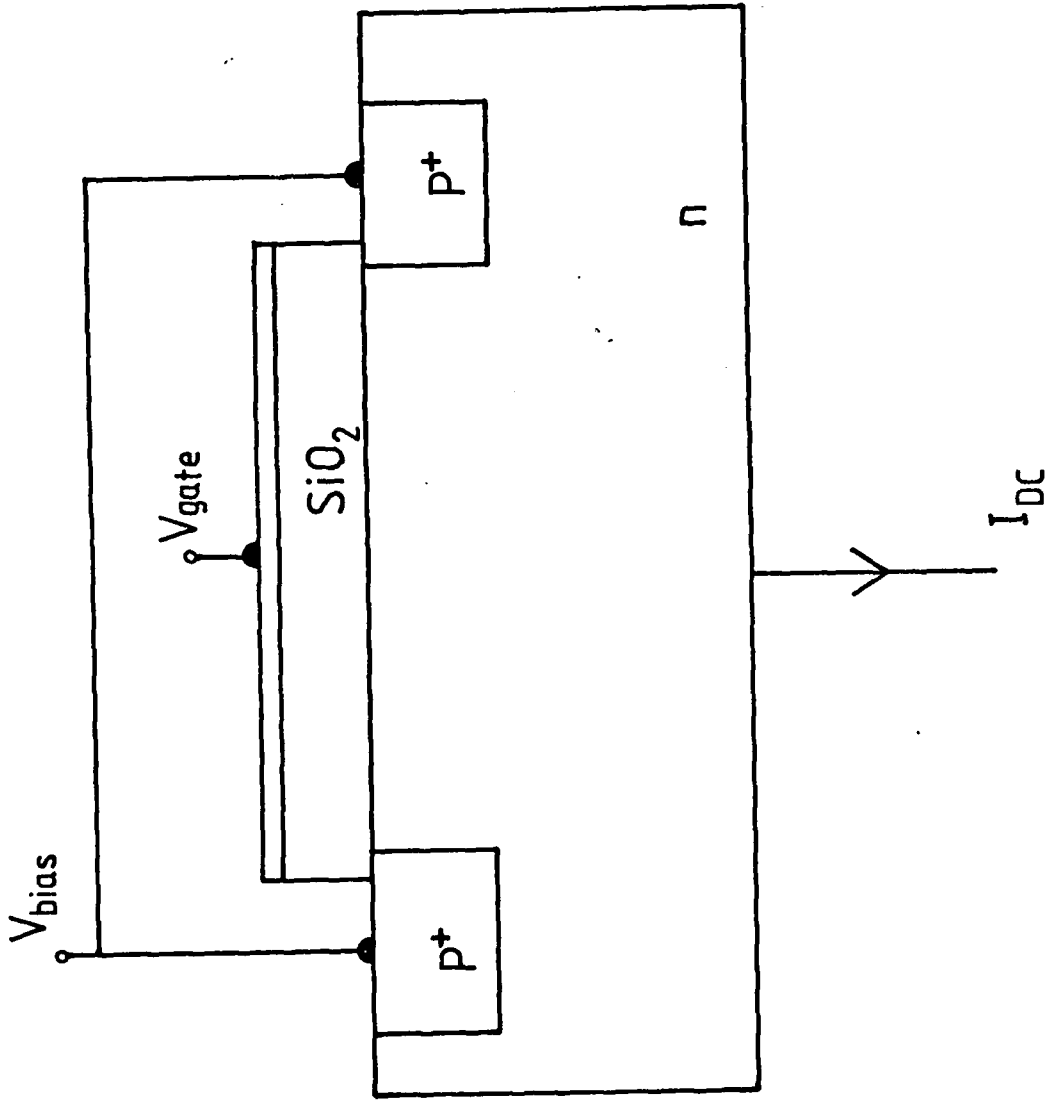


FIG. 2

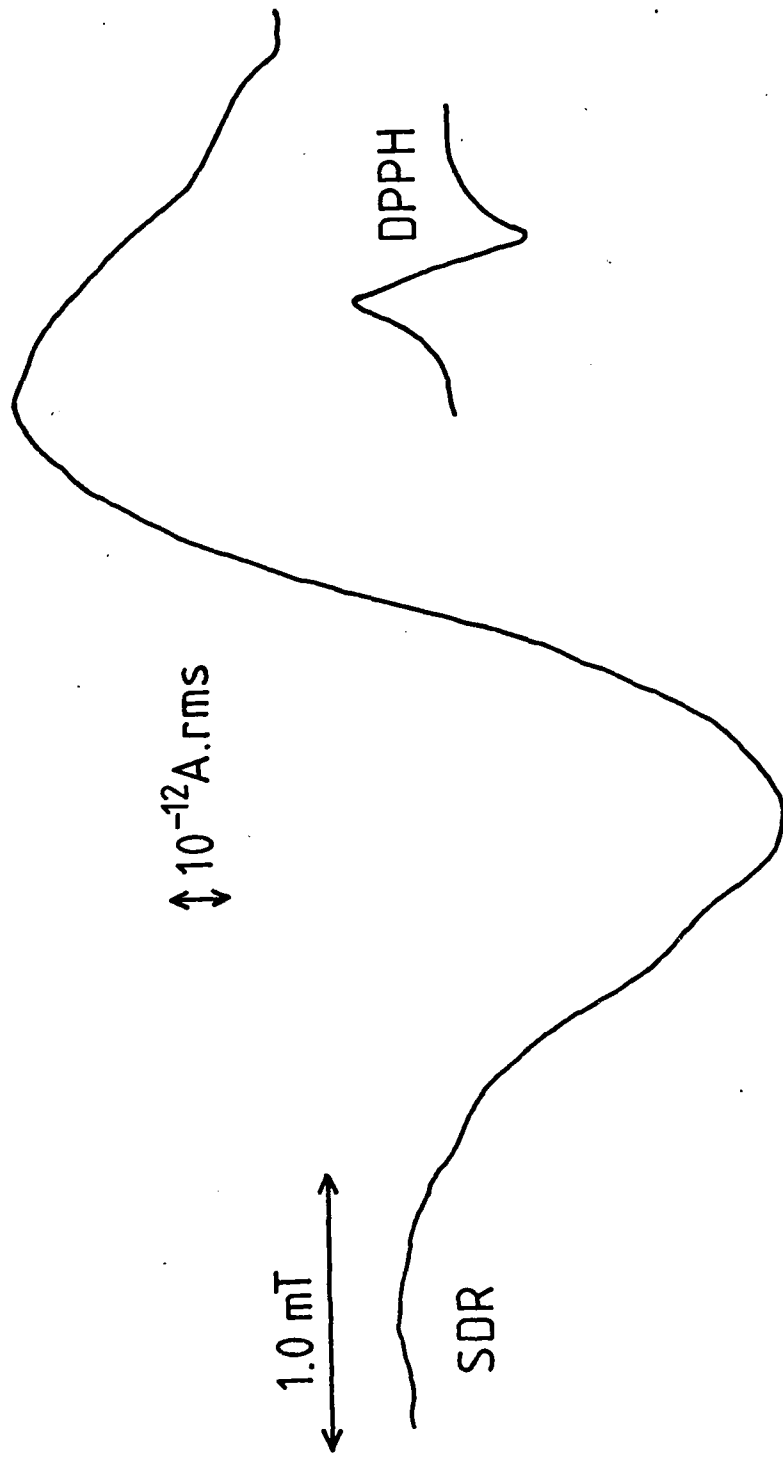


FIG. 3

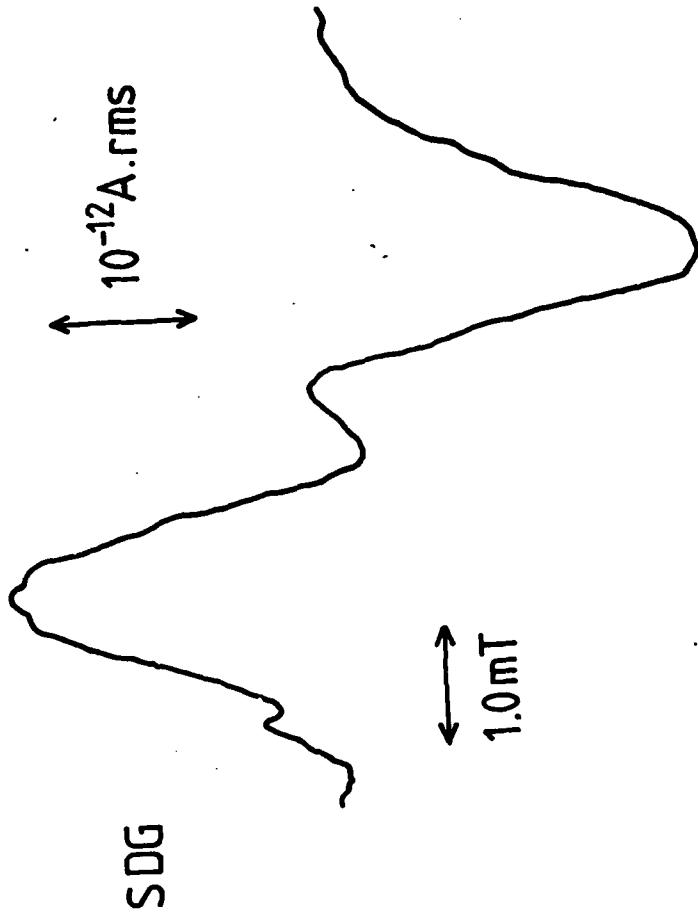


FIG. 4

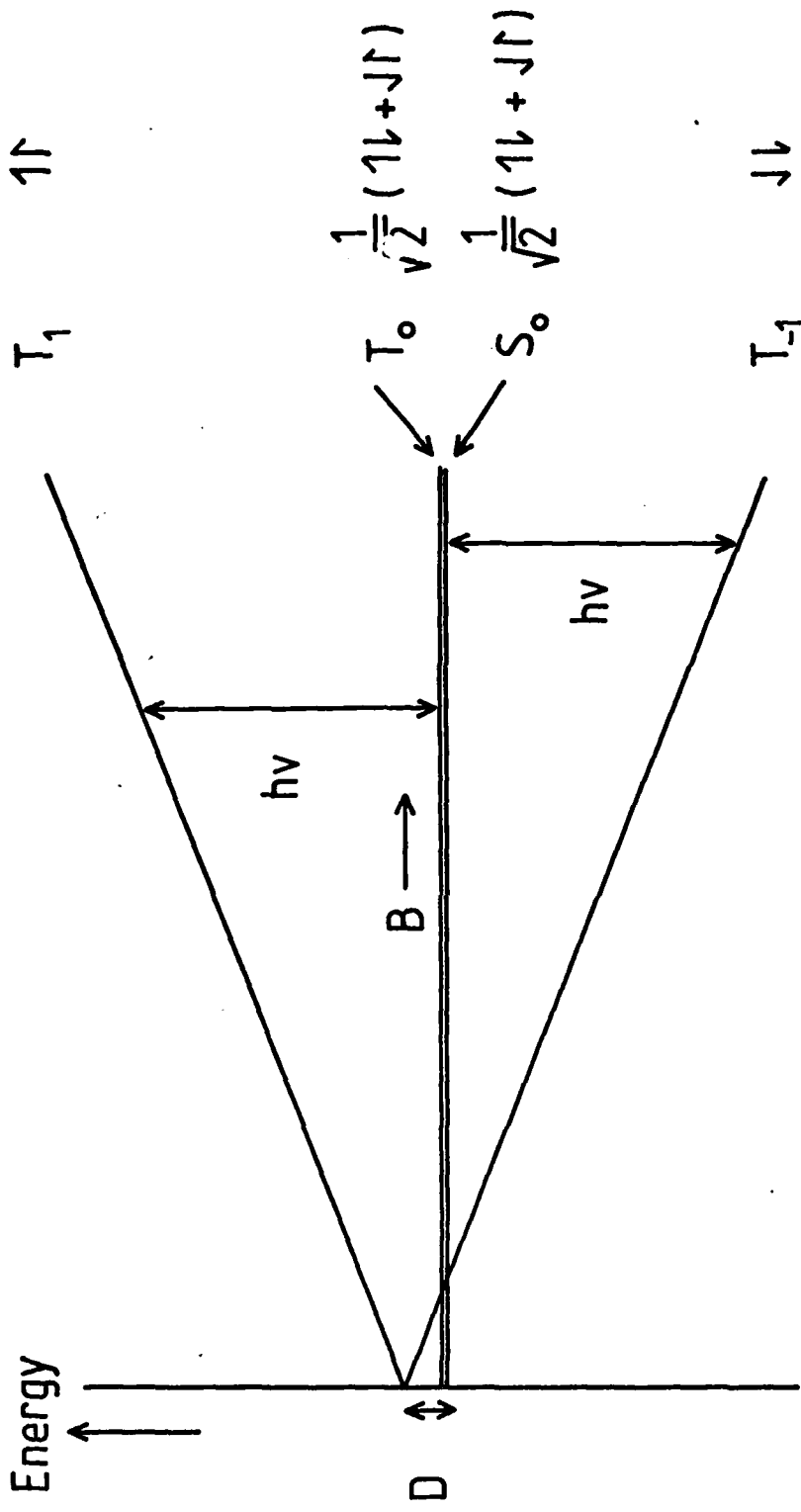


FIG. 5

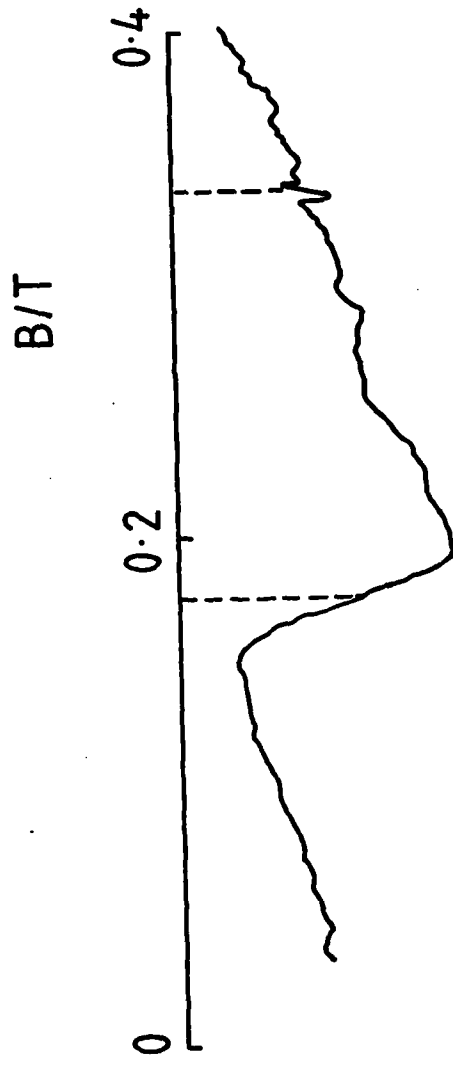


FIG. 6

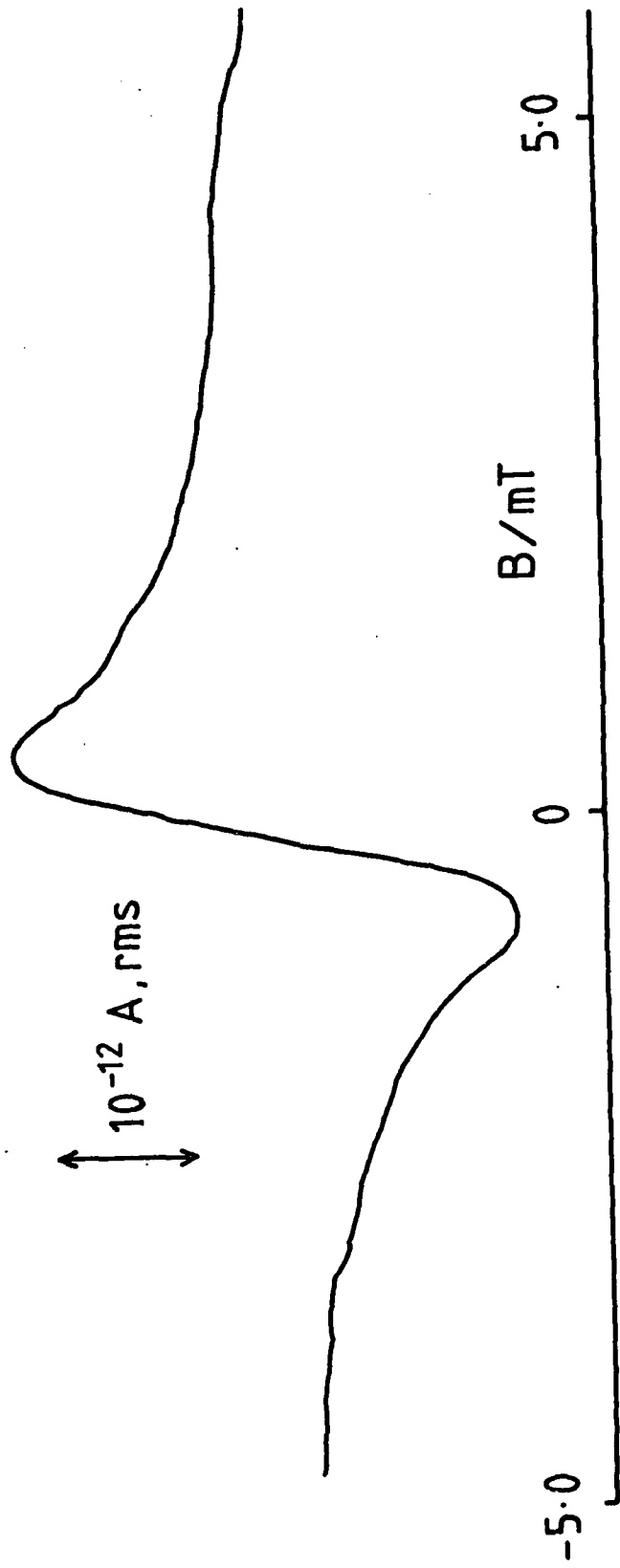


FIG. 7

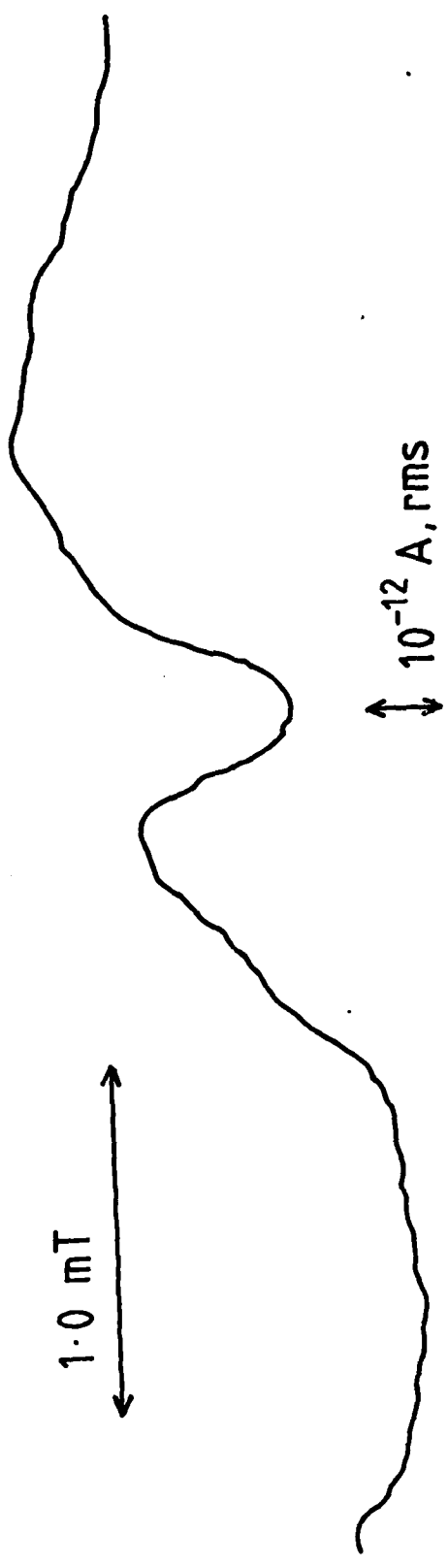
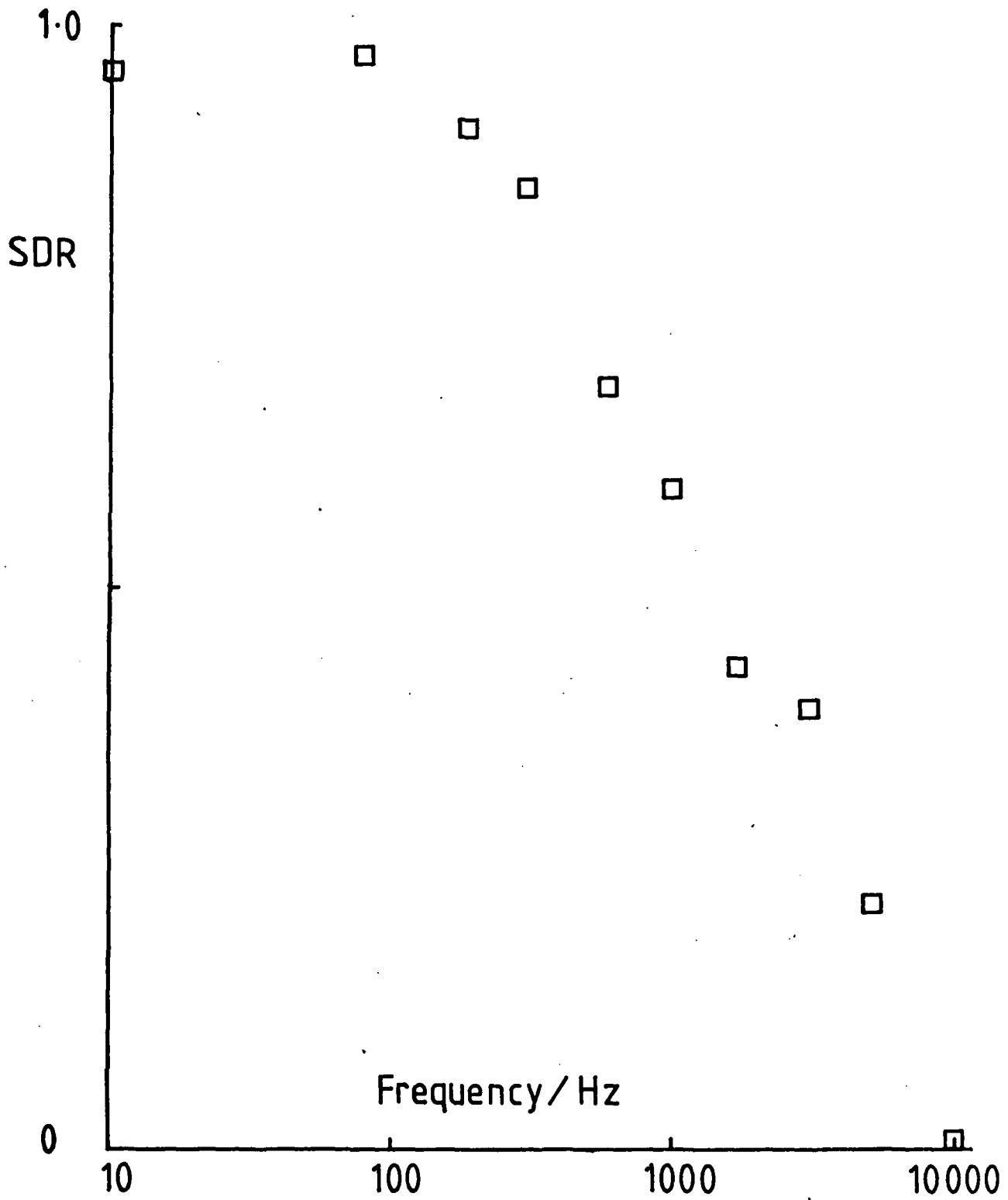


FIG. 8



FREQUENCY INDUCED ELECTRON DELOCALISATION AND FRACTIONAL QUANTISATION IN
SILICON INVERSION LAYERS

A.P. LONG^a, H.W. MYRON^b and M. PEPPER^{a,c}

a Cavendish Laboratory, Cambridge, U.K.

b Physics Department, University of Nijmegen, Netherlands.

c G.E.C. Hirst Research Centre, Wembley, Middlesex.

ABSTRACT

We demonstrate the disappearance of plateaus of quantised Hall resistance with increasing frequency resulting in a decrease in the extent of localisation. At the highest frequencies this is accompanied by the evolution of structure corresponding to fractional quantisation. This is discussed in terms of an increased role for the electron-electron interaction as the effects of disorder diminish.

Previous work on the effects of frequency on the Quantum Hall Effect demonstrated the relation between disorder induced localisation and the QHE. When states near the centre of the Landau level were weakly localised, ie, the localisation length is long, the electrons behave as if extended as the frequency is increased. The cause of this lies in the low velocity of the orbit eF/B which under the conditions used is in the range 10^2 - 10^3 cms sec^{-1} . The effect of localisation in the tails of the Landau levels is to increase this velocity in order to maintain quantisation of the Hall resistance. Nevertheless the increase in velocity is not sufficient to give a drastically increased amplitude of drift length. Earlier work (Pepper and Wakabayashi, 1982 and Pepper and Wakabayashi 1983) demonstrated that the sample length cut off the localisation and when the drift length was less than this the frequency started to produce a plateau of quantised resistance. Similar results were obtained by producing effective delocalisation with increasing temperature.

In this letter we give further evidence that states in the tails of the Landau levels are effectively delocalised at high frequencies so destroying the quantised Hall resistance. In the tails the effective length scale is determined by the diffusion coefficient, D , of the electrons and hence the rate at which they jump between localised states. As we do not know the density of states at E_F , we cannot estimate D . Measurements have been carried out on Corbino and Hall geometry MOSFET's on the (100) Si surface, the peak mobilities at 4.2K were in the range 10^4 - $1.2 \cdot 10^4$ $\text{cm}^2\text{volt}^{-1} \text{sec}^{-1}$.

Measurements on the Hall devices use two terminals exploiting the quantised magneto-resistance (Fang and Stiles, 1983; Powell et al, 1984). Figures 1 and 2 show the relation between σ_{xx} and gate voltage V_g , (1 volt= 1.7×10^{11} ecm^{-2}) for the ground Landau level. The effect of increasing frequency is to decrease the zero conductivity region, ie, the number of immobile carriers, this is illustrated in more detail in Figure 3. Figures 1 and 2 also show the increase

in the peak values of σ_{xx} with increasing frequency, this effect is illustrated in Figure 4. Another aspect of Figures 1 and 2 is the small lowest valley, lowest spin level and the structure between levels which is removed by increasing the frequency. Similar structure was reported by Tsui (1977) who found that it was removed by increasing the electric field, in this respect both field and frequency produce delocalisation.

We now present our results on the two terminal measurements of quantised magneto-resistance on Hall geometry devices $400\mu\text{m}$ long by $50\mu\text{m}$ wide. These devices were first used in the first paper announcing the discovery of the Q.H.E. (von Klitzing, Dorda and Pepper, 1980). Figure 5 shows the effects of increasing the frequency on the $i=4$ plateau ($\sim 6.38\text{k}\Omega$); it is clear that the plateau is destroyed by increasing the frequency as found earlier by Pepper and Wakabayashi. The finite response of the electrons in the tails of the Landau level results in the quantised value being found only when E_F is between empty and filled levels, ie $N(E_F)$ is zero and no a.c. response is possible. There appears to be a critical frequency for this which is sample dependent, we have not investigated the dependence on sample length but we would expect this to be present. The decrease in plateau width is consistent with the reduction in the number of immobile electrons illustrated in Figure 3. This is clear evidence for the role of the frequency in removing localisation so narrowing and finally eliminating the plateau of quantised resistance. Being a *manifestation* of localisation the Q.H.E is essentially a d.c. effect.

We now show in detail measurements of the V_g dependence of two terminal conductance, G , in a magnetic field of 25 Tesla, Figures 6 and 7. Due to cable losses there is an overall change which we have not corrected. The essential features are the loss of the integer quantised plateaus and the appearance of structure. This structure is strongest below the

spin gap and its evolution as a function of frequency is shown in Figure 7. In Figure 8 the decrease in the integer plateau and the formation of this structure is clear. Figure 9 shows that the structure shifts with magnetic field in the same way as that corresponding to the integer Q.H.E. indicating that it is related to filling factors $4/3$ and $5/3$ although the ratio of the $5/3$ and 2 peaks is $.72$ rather than the expected $.833$ indicating that the $5/3$ peak has not completely developed with increasing frequency. This result is expected as the decreased role of disorder and localisation will increase the role of the electron-electron interaction. We note that the role of the disorder in giving a plateau based on the interaction gap is itself minimised by frequency so tending to give a fractional peak rather than a plateau.

In summary we have demonstrated that increasing the frequency, and decreasing the length scale of transport, minimises the role of disorder and localisation so converting a plateau of quantised Hall resistance into a peak. When the localisation is sufficiently small the increasing influence of the electron-electron interaction results in the formation of fractional quantisation as in GaAs under d.c. conditions (Tsui et al 1982).

ACKNOWLEDGEMENTS

We have enjoyed many discussions with J.W. Wakabayashi, C. McFadden, T. Powell and C.C. Dean. We are grateful to the technical staff of the high magnetic laboratory, University of Nijmegen for their valuable assistance.

This work was supported by S.E.R.C., in part by the European Research Office of the U.S. Army and a N.A.T.O. travel grant.

REFERENCES

1. Fang F.F. and Stiles P.J., Phys. Rev. B27, 6487, 1983.
2. Pepper M. and Wakabayashi J., J. Phys. C 15, L861, 1982.
3. Pepper M and Wakabayashi J., J. Phys. C 16, L113, 1983.
4. Powell T.G., Dean C.C. and Pepper M. J. Phys. C. 17, to be published.
5. Tsui D.C., Solid State Communications 21, 675, 1977
6. Tsui D.C., Stormer H.L., Gossard A.C., Phys. Rev. Lett., 1559, 1982
7. von Klitzing K., Dorda G. and Pepper M., Phys. Rev. Lett. 45, 494, 1980.

FIGURE CAPTIONS

Figure 1 The real part of the conductivity σ_{xx} as a function of the gate voltage V_g for a Corbino geometry. The frequency of the electric field $E_{sd} = 75 \text{ mV/cm}$ (R.M.S) is 500kHz. The magnetic field $B = 14.4$ Tesla and the temperature $T = 1.4\text{K}$.

Figure 2 The real part of the conductivity σ_{xx} as a function of the gate voltage V_g at a frequency of 40 MHz.

Figure 3 Plot of the number of immobile electrons in the spin gap (x) and Landau level gap (0) in the ground Landau level as a function of frequency for sample P2C8. $B = 14.4$ Tesla, $T = 1.4\text{K}$ and $E_{sd} = 75 \text{ mV/cm}$ (R.M.S).

Figure 4 The frequency dependance of the heights of the four conductivity peaks in the ground Landau level, (o) is $0\downarrow-$, (Δ) is $0\downarrow+$, (\blacktriangle) is $0\uparrow-$ and (o) is $0\uparrow+$.

Figure 5 Detail of the $i = 4$ step (ground Landau level) of the quantised Hall resistance in a $400\mu\text{m}$ long $50\mu\text{m}$ wide Hall geometry sample at various frequencies. The magnetic field $B = 7$ Tesla the temperature $T = 1.2\text{K}$ and the electric field $E_{sd} = 75 \text{ mV/cm}$ (R.M.S.)

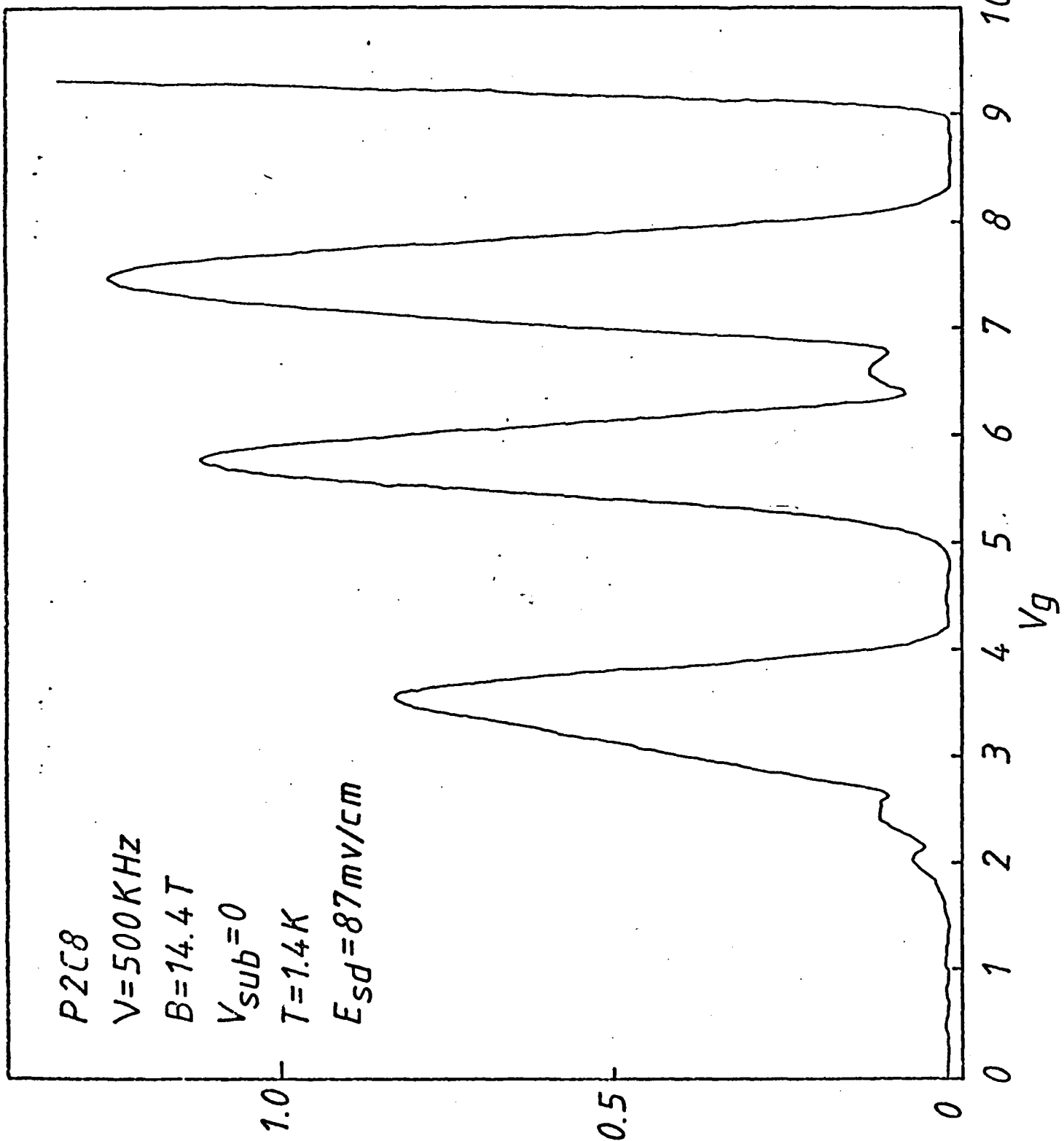
Figure 6 The two-terminal quantised Hall resistance at 500 kHz and 5 MHz. The magnetic field $B = 25$ Tesla, the temperature $T = 1.3\text{K}$ and the electric field $E_{sd} = 75 \text{ mV/cm}$ (R.M.S.)

Figure 7 The two-terminal quantised Hall resistance at 20MHz and 45MHz.
The evolution ^{with frequency} of extra structure between peaks 1 and 2 is seen.

Figure 8 Detail of the region of the first two steps in the quantised Hall resistance showing the reduction in the integer steps and the appearance of extra structure at the highest frequencies.

Figure 9 The magnetic field dependence of the structure at Landau level filling factors of $4/3$ and $5/3$.

Figure 1



75 01/18/80

Figure 2

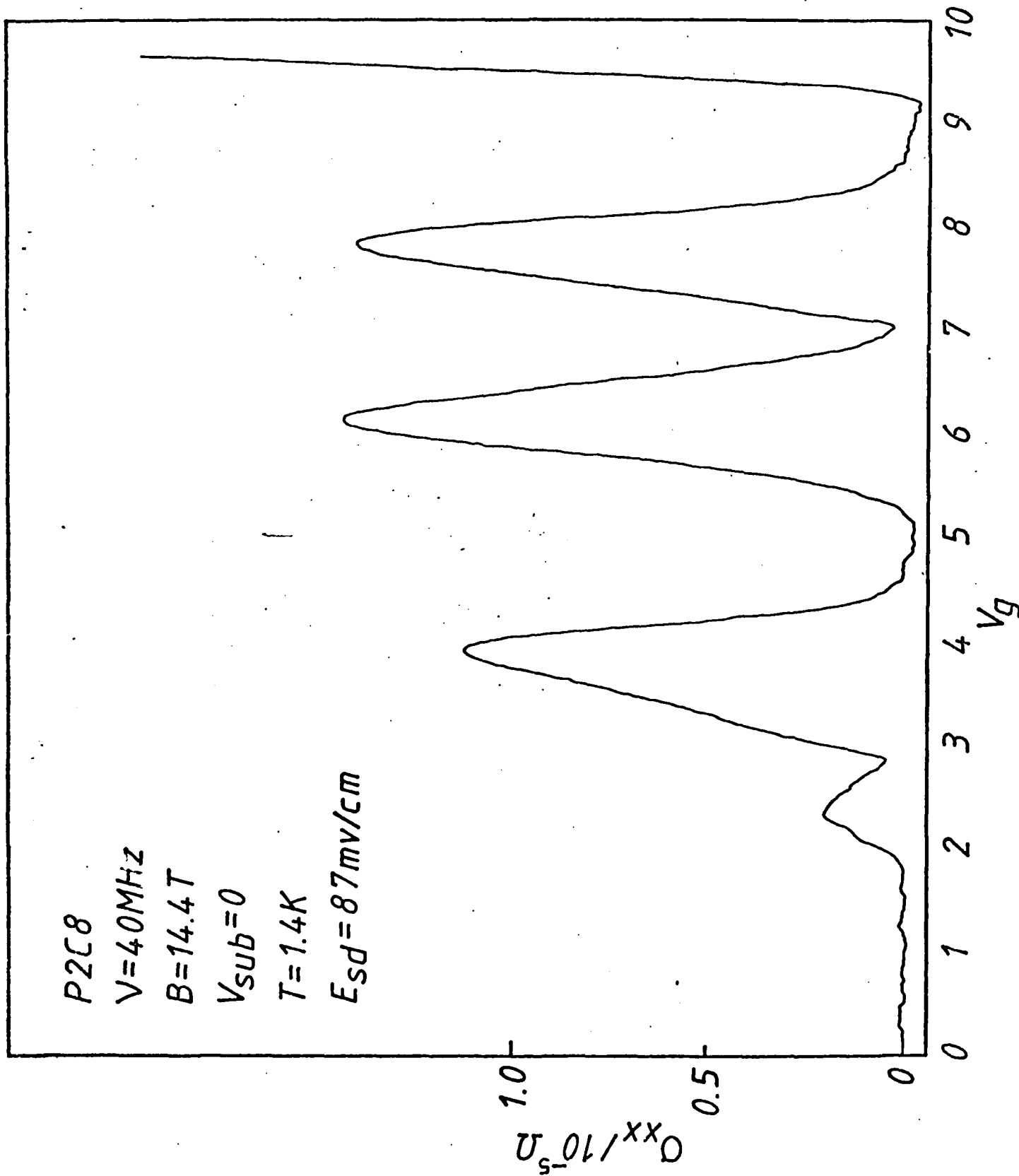


Figure 3

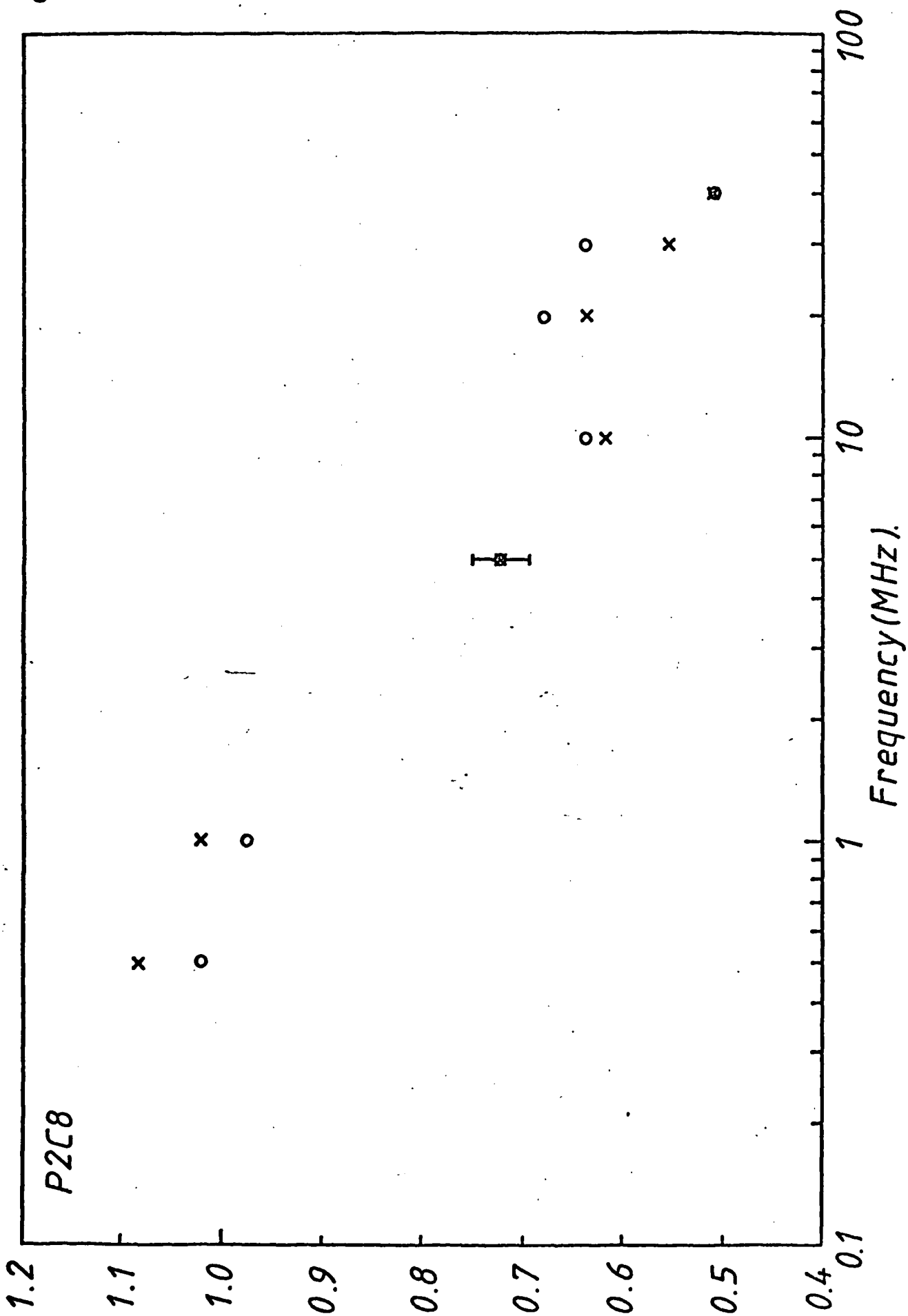


Figure 5

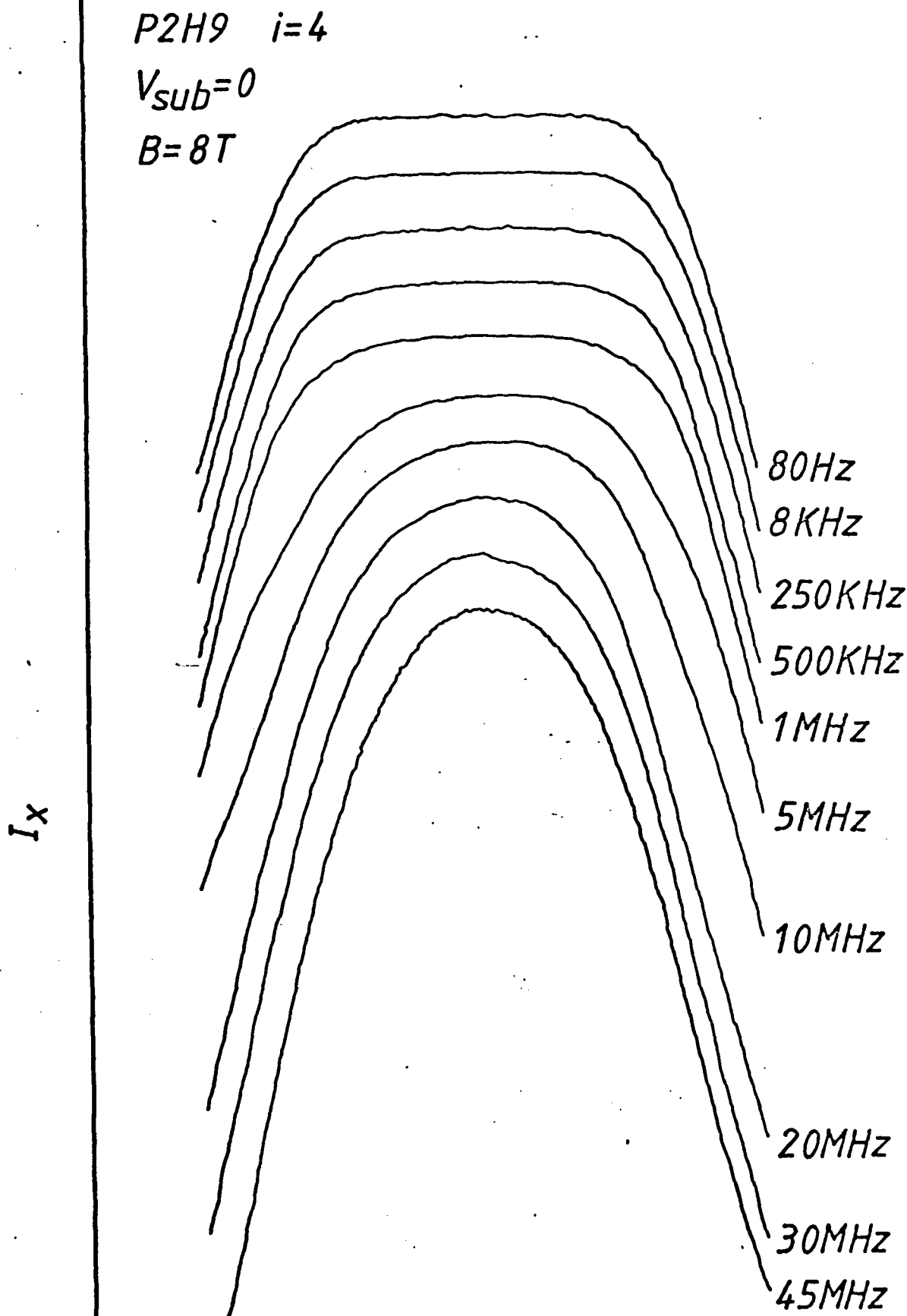


Figure 6

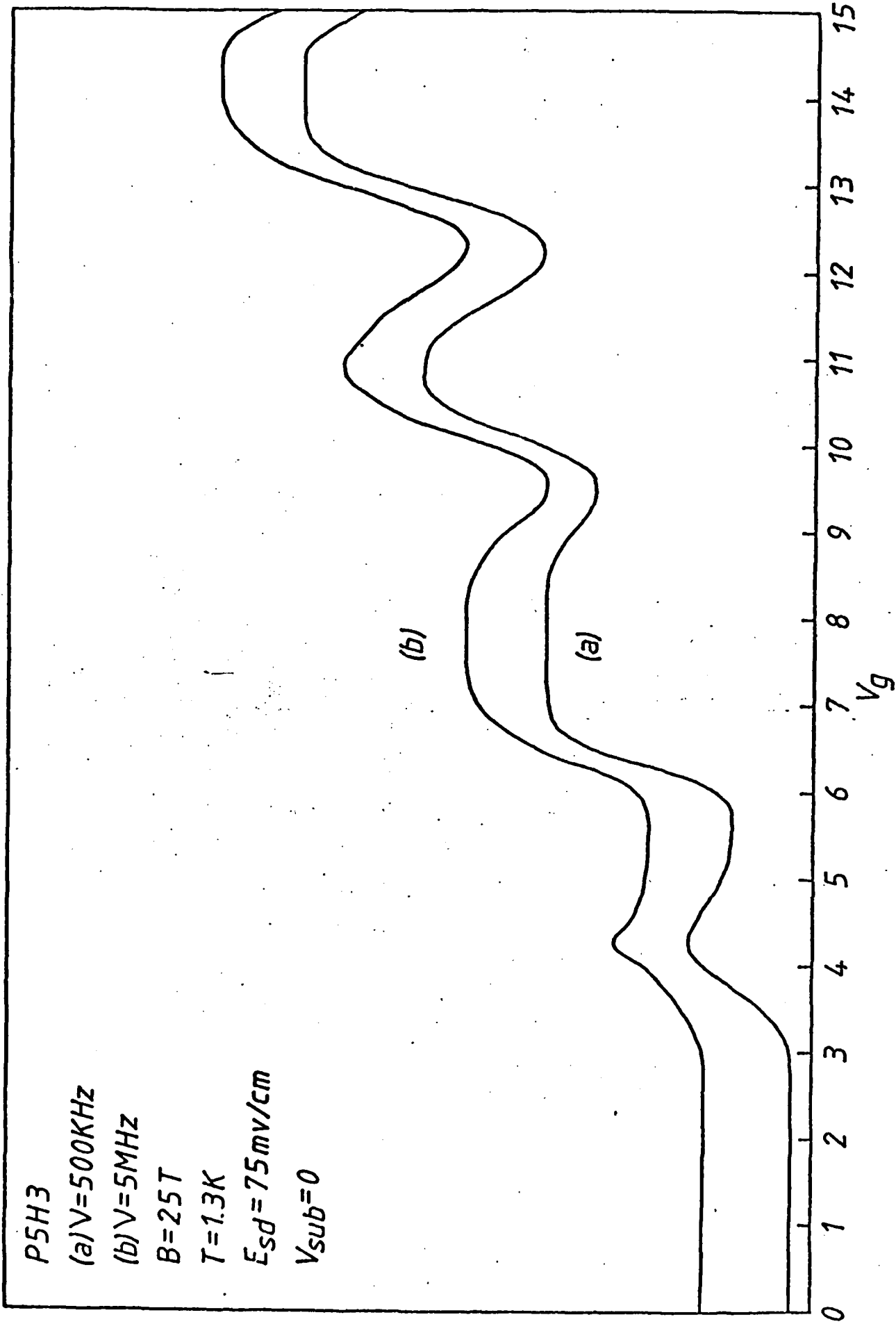


Figure 7

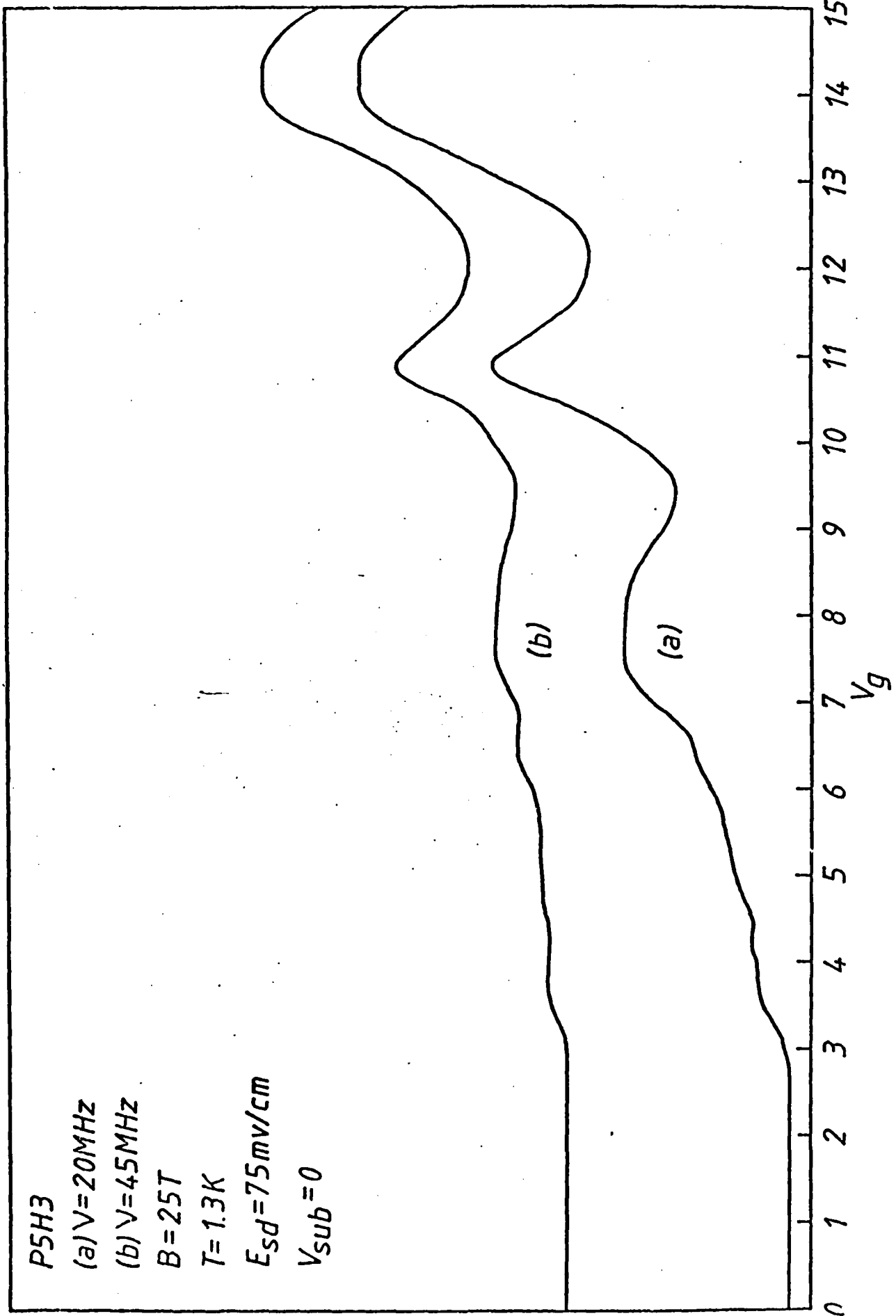


Figure 8

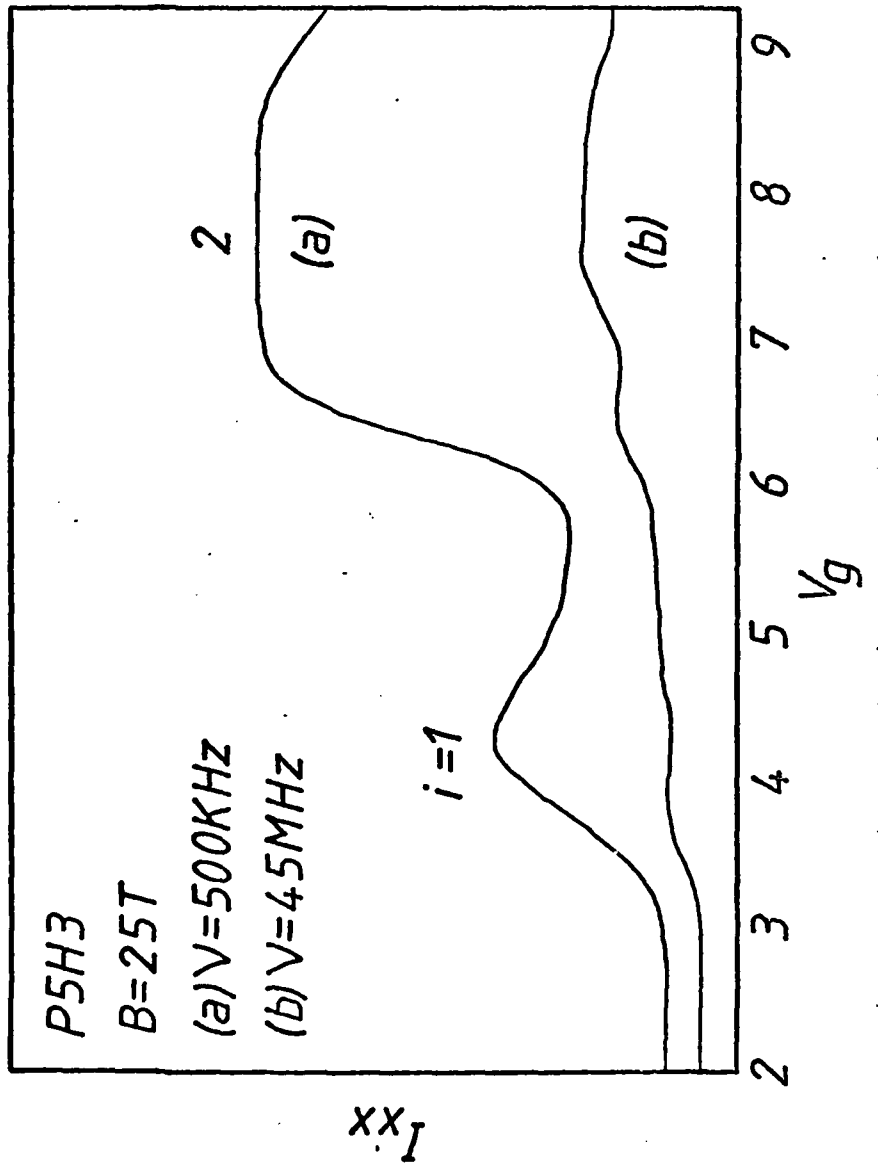
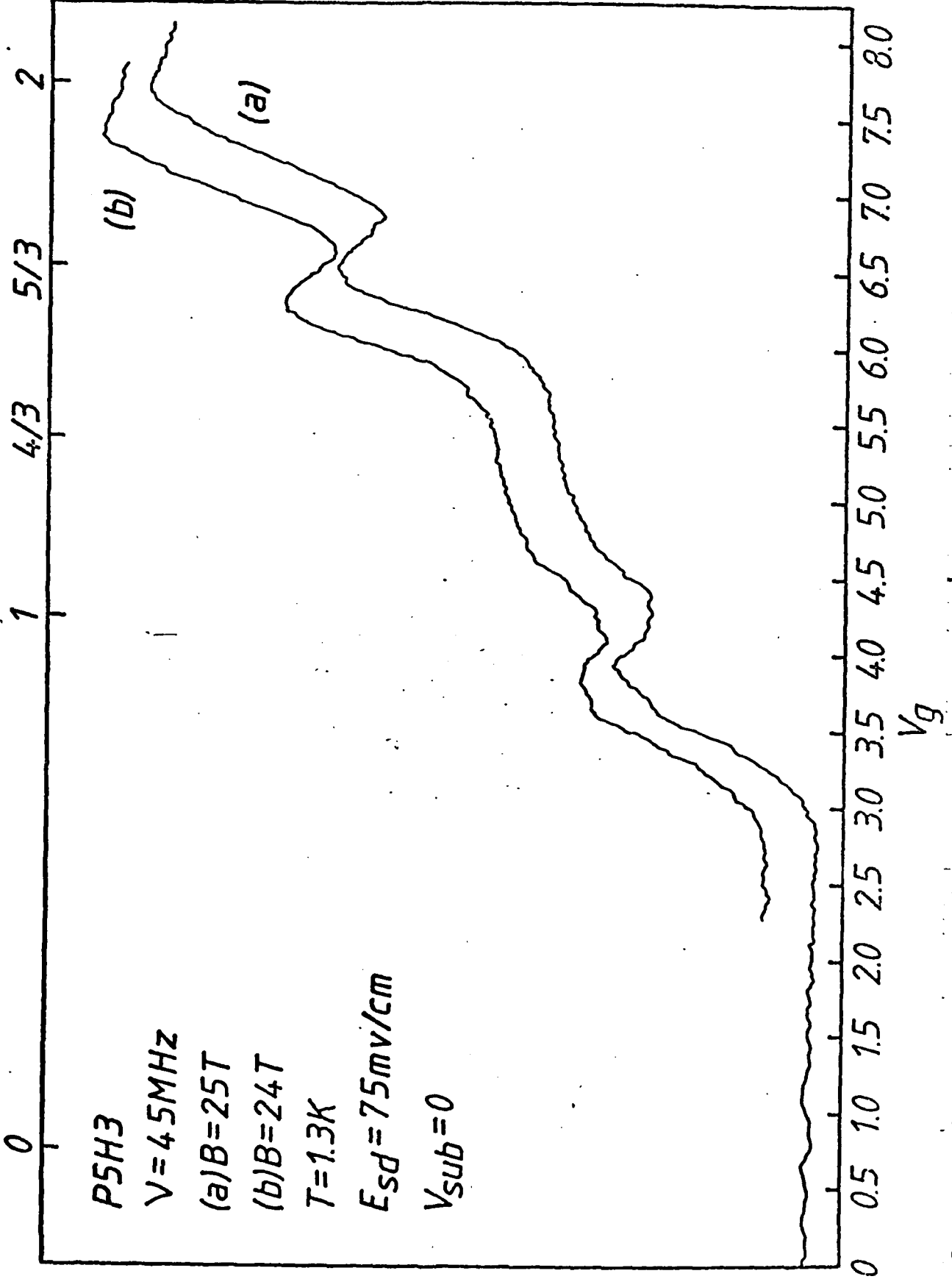


Figure 9

FILLING FACTOR ($B=25T$).



xx1

FREQUENCY ENHANCED FRACTIONAL QUANTISATION IN GaAs-GaAlAs HETEROJUNCTIONS.

by

C.McFadden^(a) ,A.P.Long^(a) ,H.W.Myron^(b) ,M.Pepper^(c) ,
G.J.Davies^(d) and D.Andrews^(d).

(a) Cavendish Laboratory,University of Cambridge,Madingley Road,Cambridge
CB3 0HE,U.K. .

(b) Physics Department,University of Nijmegen,Netherlands.

(c) Cavendish Laboratory and G.E.C.Hirst Research Centre,Wembley,Middlesex.

(d) British Telecom Research Centre,Martlesham Heath,Ipswich.

ABSTRACT

We report the observation of fractional quantisation obtained by increasing the frequency of measurement,this is found up to a Landau index of 10. The result is coincident with the suppression of integer quantisation and is interpreted as indicating a transition from a liquid state to a solid state behaviour as the time scale of measurement is reduced.

Previous work has established that varying the frequency of measurement has a pronounced effect on the measurement of the Quantum Hall Effect (Q.H.E.) (Pepper and Wakabayashi, 1983; Wakabayashi, Myron and Pepper, 1983; Long, Myron and Pepper, 1984). This arises from the Q.H.E. being a manifestation of localisation in the Landau level. If states at the centre of the level are weakly localised, plateaus of quantum Hall resistance are not found at d.c. However if the frequency of measurement is increased, then when the amplitude of the drift path of the centre of the orbit is less than the localisation length, the plateaus of quantised Hall resistance become apparent. The frequency aided delocalisation occurs first at the centre of the Landau level where localisation is weakest. Further increase in frequency delocalises states in the tails of the Landau levels so destroying a necessary condition for the observation of the Q.H.E. The exact increase in frequency necessary for the observation of this effect depends on the localisation length, i.e. disorder, and hence will be sample dependent. Previous work (Pepper and Wakabayashi, 1983) has indicated that the maximum observable localisation length is the sample length, which acts as a cut-off. The previous work showed that increasing the frequency removed the plateau by delocalising tail states and the quantised value was only found when E_f was between empty and full Landau levels - the condition for the quantisation in the absence of localisation. The essential feature of the 'frequency effect' is that when the sample is in the plateau condition the velocity of the centre of the orbit is F/B , where F is the Electric Field and B is the magnetic field. However if a number of carriers are localised then the velocity is correspondingly increased to maintain the quantisation of Hall resistance, this can result in a considerable increase in the velocity as a substantial proportion of the carriers can be localised. In

that the velocity enhancement was no more than a factor of three. A typical velocity of electrons in the plateau of the ground Landau level is 10^2 cm sec^{-1} , at a frequency of 10 MHz, this gives a drift length of 150 Å. In the tails of the levels rough estimates of the diffusivity D , suggest that the diffusion length in a frequency ω can be decreased considerably using the MHz region of frequencies. This is particularly effective as the localisation lengths are long. Accordingly we would expect the a.c. conductivity to be less dependant on scattering and disorder and be more dependant on the electron-electron interaction than under d.c. conditions. We therefore investigated the possibility of using the effect of frequency to observe the Fractional Quantum Hall Effect (Tsui et al. 1982, Stormer et al. 1983, Laughlin 1983)

The samples used in this experiment were MBE grown modulation doped GaAs-GaAlAs heterojunctions in the form of gated Hall bars, 1.9mm long and 0.2mm wide. The mobility, μ , and carrier concentration, n_s , could be continuously varied between 120,000 cm^2/Vs at $n_s = 5 \times 10^{11}$ $\text{e}^- \text{cm}^{-2}$, to 50,000 cm^2/Vs at $n_s = 2.7 \times 10^{11}$ $\text{e}^- \text{cm}^{-2}$. Lock-in techniques were used to measure only the in-phase component of current from a matched current monitoring resistor and the two terminal conductance method of measurement was used (Fang and Stiles, 1983; Powell et al; 1984). Our method of measurement eliminated the role of gate capacitance but we experienced cable loss, here we compensated for the loss at those frequencies where it occurred. The frequency dependent magneto-conductance oscillations were measured at $T=1.4\text{K}$ in fields up to 20 Tesla.

An example of the d.c. Quantum Hall Effect obtained at 280 mK is shown in Fig.1 ; as seen the integer plateaus are very broad down to $i=2$, the field available was not high enough to observe the $i=1$ plateau. Figure 2 shows the high field two terminal conductance obtained at 1.4K and 80Hz. Here the $i=1$ and 2 plateaus are observable but the higher temperature prevents a clear

plateau for $i=3$, which is a spin split state. On figure 2 we have indicated the expected positions of the plateaus and it is clear that there is no additional structure. Figure 3 shows G_{2T} plotted against magnetic field for frequencies upto 5MHz. At frequencies upto 1 MHz the $i=1$ and $i=2$ plateaus have their expected values and additional structure appears at a filling factor $\nu = 4/5$. With further increase in frequency the $i=2$ plateau remains flat upto 2.5 MHz but falls in value. This is due to cable loss and we find that the loss increases linearly with frequency and can be modelled by a parasitic capacitance of 0.8pF. This enables us to extract the two terminal device conductance G_{2T} . It is clear that fractional quantisation is present at filling factors $\nu=5/3$ and $\nu=4/5$, the structure at $4/5$ being a plateau at the correct value of conductance at 5 MHz. A distinct feature of the result is the collapse of the $i=1$ integer plateau, this has disappeared at 5 MHz and becomes a minimum at higher frequencies. At frequencies higher than 2.5 MHz the $i=2$ plateau starts to disappear and becomes a minimum. At 10 MHz there is evidence of further structure (Fig.4) but this is not analysed here. Increasing the frequency to 20 MHz results in a pronounced minimum at $i=2$, appreciable loss was found at this frequency preventing analysis of lower order structure.

The frequency was found to have a pronounced effect on higher order Landau levels. The principal structure was always at the $2/3$ filling factors and this was apparent up to $\nu=32/3$ which occurred at a magnetic field of 1 Tesla. Figures 5a and 5b show the Landau level indexation at frequencies of 500kHz and 10 MHz. It is seen that at low frequencies only integer quantisation is present but at higher frequencies the fractions are dominant. It is noticeable that when an integer peak appears strongly localised, and does not reach a quantised value at low frequency, it is not significantly affected by frequency and persists when other integers have disappeared. This is most pronounced for odd integers which being spin split

are the weakest, and is exemplified by the persistence of the $i=3$ peak. Figure 6 illustrates the progressive decline of the $i=4$ and 6 integer peaks and the appearance of the $11/3$ and $17/3$ peaks.

We have investigated these effects as a function of carrier concentration, n_s , which is varied by the gate voltage. The enhancement of the fractions and decrease of the integer peaks by frequency, is most pronounced as n_s decreases, this is despite the decrease in mobility. Presumably the frequency is minimising the disorder element and the reduction in n_s is increasing the relative importance of the interaction for a given filling factor.

We now turn to a discussion of the main points of this work, namely the frequency induced appearance and enhancement of the fractional quantisation and coincident decrease and collapse of integer quantisation. The essential feature of the experiment is that the diffusion length of the electrons is smaller than the localisation length. The drift length of the extended electrons is small and we therefore remove the role of localisation lengths greater than this. We expect as in Si, the conversion of the quantised plateau to a peak as frequency is increased. However, the results go beyond this and the integer quantisation disappears and then becomes a minimum. We conclude that this is the result of electron interactions which is also producing the fractional quantisation. The frequency is enhancing the liquid state and the interaction. Our measurement is monitoring the response of the electrons over a short period of time ($1/\omega$) and it appears as if the entire Landau level does not conduct for very short intervals of time (10^{-8} s). The observation of an insulating state when the time is short suggests that when E_f is between Landau levels the system behaves as a pinned solid and is an insulator. As the time increases the liquid state becomes apparent giving conduction and the integer quantisation reappears. It is the liquid motion itself which gives diffusion and conduction.

We therefore conclude that at very short intervals of time, or insignificant disorder, conventional (integer Landau level) magnetic quantisation will not be observed. The only quantisation apparent will be at fractional values and transport is totally dominated by mutual interactions of electrons.

The results suggest that in any Landau level the interaction increases as the filling factor increases. Thus the integer disappears and the $2/3$ occupancy is favoured over $1/3$ etc. There is a complicated relation between disorder, interactions and frequency. The disorder and localisation, gives a plateau based on the interaction induced fractional gap. Increasing frequency enhances the gap, but also minimises the plateau by reducing the disorder induced localisation. Therefore we expect the system will behave as a solid at sufficiently high frequencies and for all values of carrier concentration.

ACKNOWLEDGEMENTS

We have enjoyed many discussions with Dr. J. Wakabayashi and Dr. D. Woods. This work was supported by S.E.R.C., in part by the European Research Office of the U.S. Army and we acknowledge a N.A.S.O. travel grant. C. McFadden and A. P. Long acknowledge S.E.R.C. grants. C. McFadden also acknowledges a G.E.C. (CASE) studentship. We are grateful to the technical staff of the High Magnetic Field Laboratory, University of Nijmegen for their assistance.

CAPTIONS TO FIGURES

Figure 1 Shows the Quantum Hall Effect (ρ_{xy} vs B) at $f=80\text{Hz}$, $T=280\text{mK}$, $V_g=+0.2\text{v}$.

Figure 2 Shows the two terminal conductance G_{2T} vs magnetic field at $f=80\text{Hz}$, $T=1.4\text{K}$, $V_g=+0.2\text{v}$. The Landau level filling factor ν is shown on the top scale whilst the expected values of G_{2T} are shown on the r.h.s.

Figure 3 Shows the two terminal conductance G_{2T} vs magnetic field at $T=1.4\text{K}$, $V_g=0.0\text{v}$ and $f=500\text{kHz}$ to 5MHz . $n_s=2.7 \times 10^{11}\text{ cm}^{-2}$ and $\mu=5.5\text{ m}^2/\text{Vs}$. The Landau level filling factor ν is shown on the top scale whilst the expected values of G_{2T} are shown in multiples of $e^2/2\pi h$.

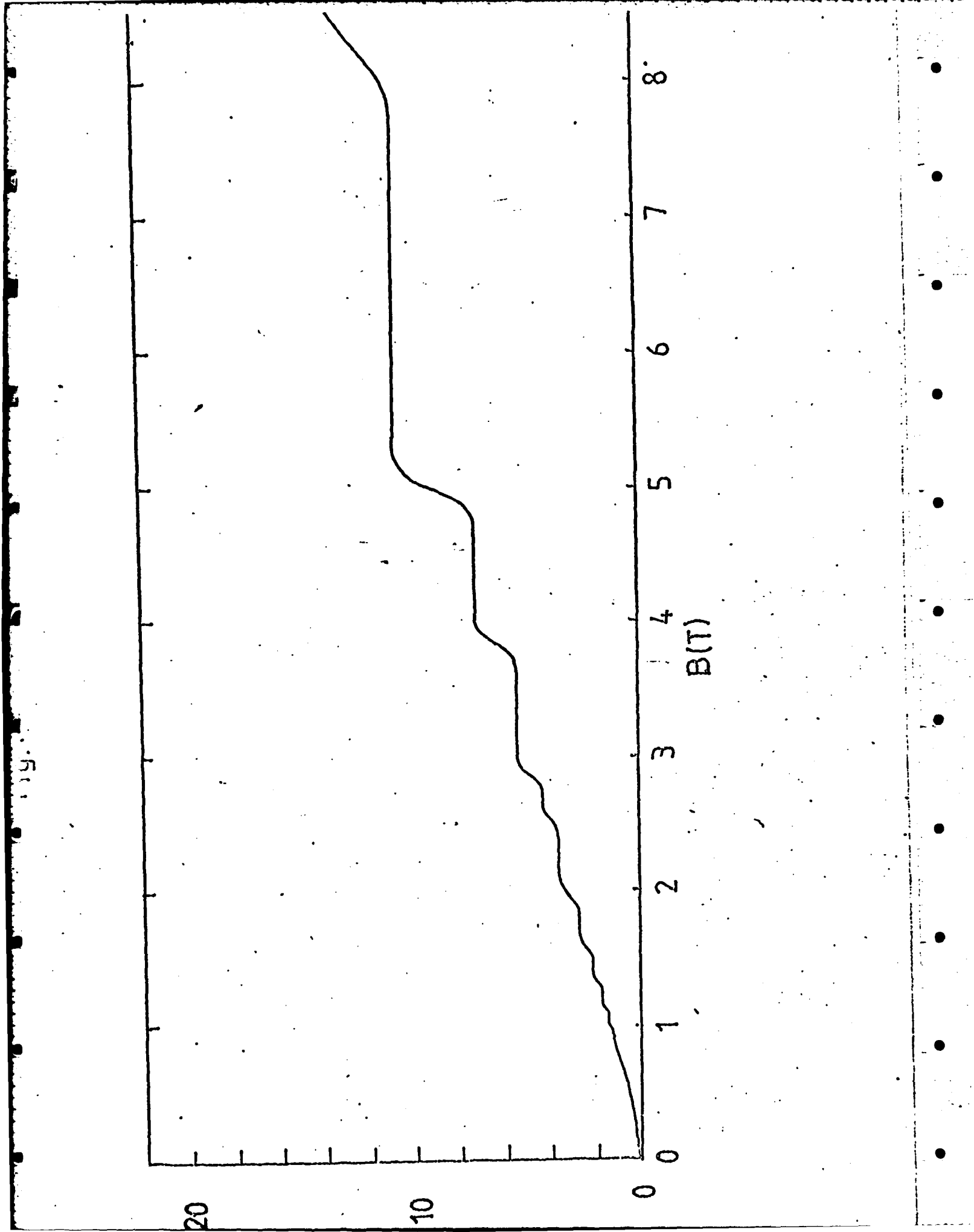
Figure 4 Shows the two terminal conductance G_{2T} vs magnetic field at $T=1.4\text{K}$, $V_g=0.0\text{v}$ and $f=10$ and 20MHz . The Landau level filling factors ν are shown on the top scale.

Figure 5 Shows the Landau level filling factor vs $1/B$ for $T=1.4\text{K}$, $V_g=0.0\text{v}$ and $f=500\text{kHz}$ (a) and $f=10\text{MHz}$ (b).

Figure 6 Shows the two terminal conductance vs magnetic field between 1.5 and 4.0 Tesla to indicate the emergence of the $17/3$ and $23/3$ peaks and the coincident suppression of the integer peaks $i=6$ and $i=4$. The graphs have been offset for clarity, for exact values refer to figures 3 and 4.

REFERENCES

1. Fang F.F. and Stiles P.J., Phys. Rev. B, 27, 6487, 1983.
2. Laughlin. Phys. Rev. Lett. 50, 1395, 1983.
3. Long A.P., Myron H. and Pepper M. - to be published.
4. Pepper M. and Wakabayashi J., J. Phys. C, 16, L113-L117, 1983
5. Powell T., Dean C.C. and Pepper M., J. Phys. C. - to be published.
6. Störmer H.L., Chang A., Tsui D.C., Hwang J.C., Gossard A.C., and Weigmann W., Phys. Rev. Letts., Vol 50, No. 24, pp1953-1955, 13 June 1983.
7. Tsui D.C., Störmer H.L. and Gossard A.C., Phys. Rev. Lett. 48, 1159, (1982).
8. Wakabayashi J., Myron H. and Pepper M., Physica 117B & 118B (1983), pp 691-693.



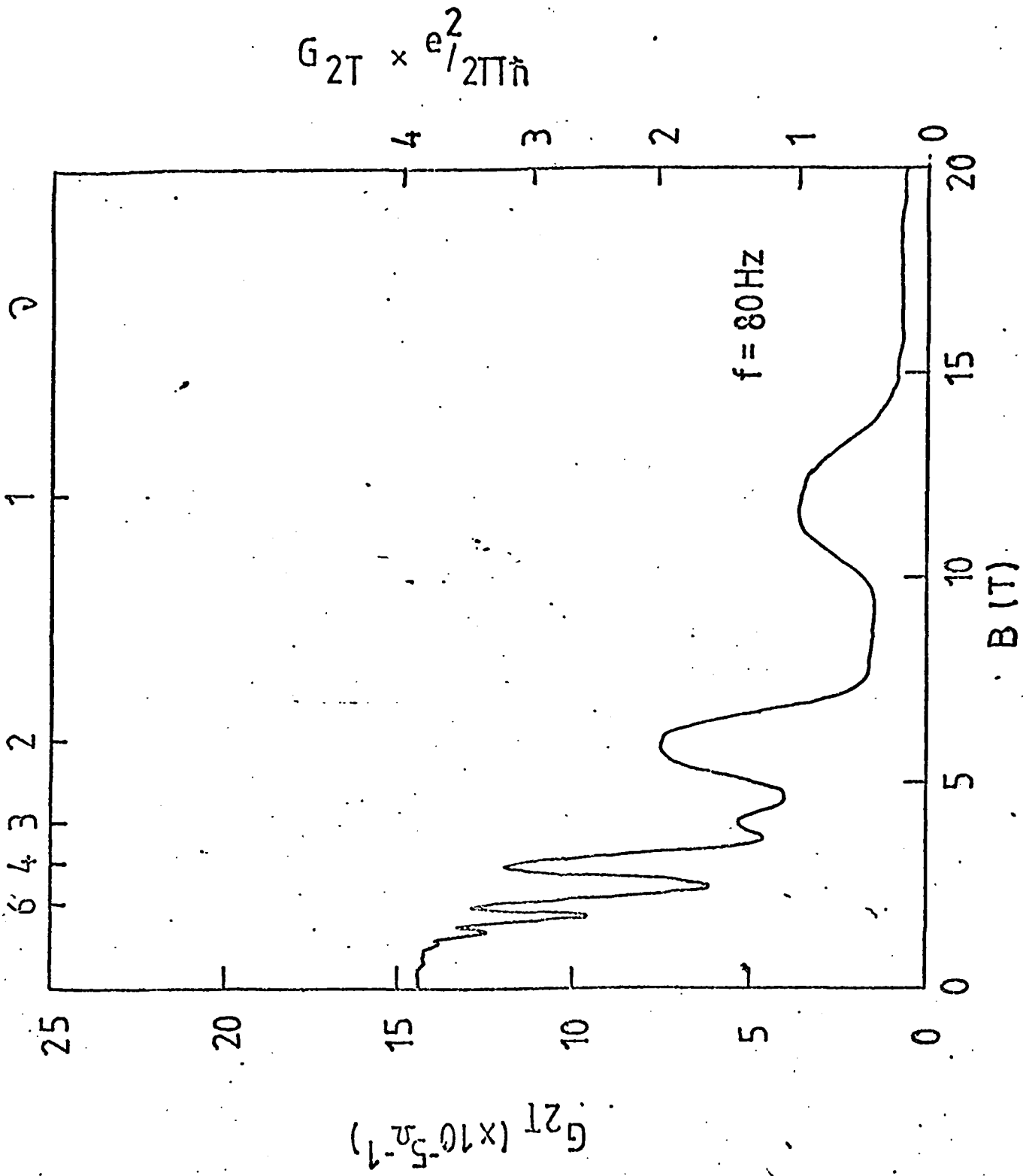
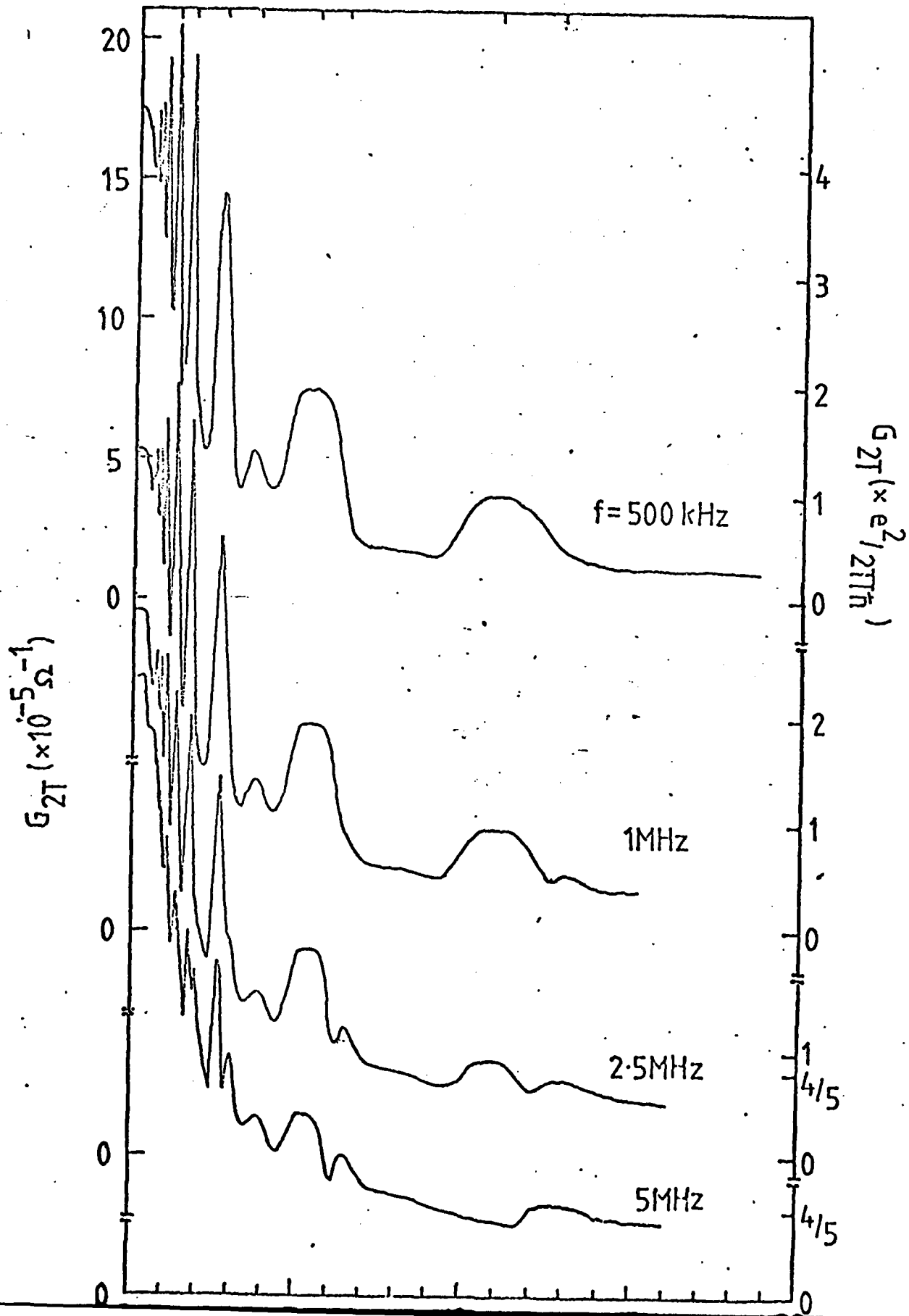


Fig. 2

86 4 3 2 ⁵/₃ 1 ⁴/₅ 0



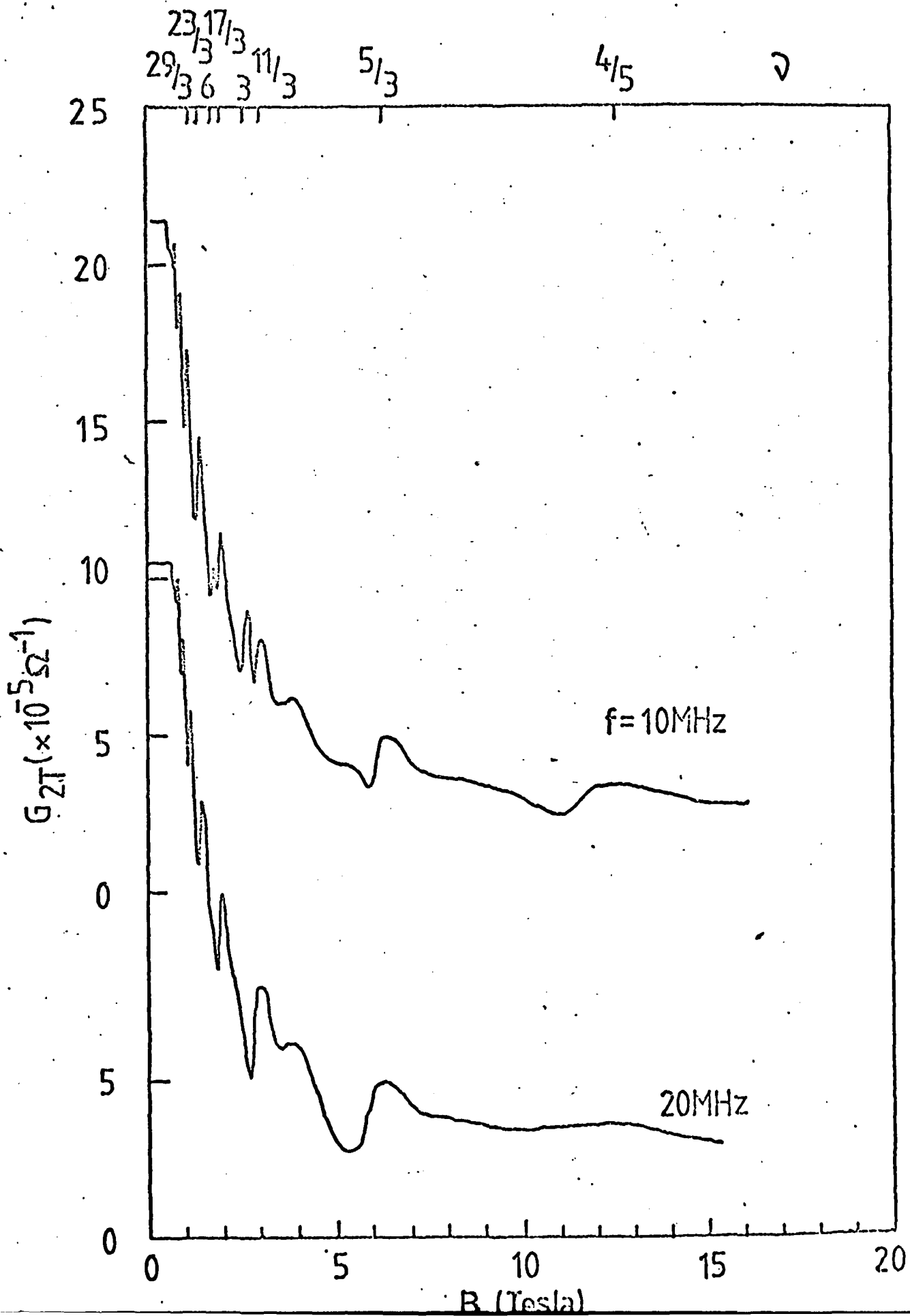
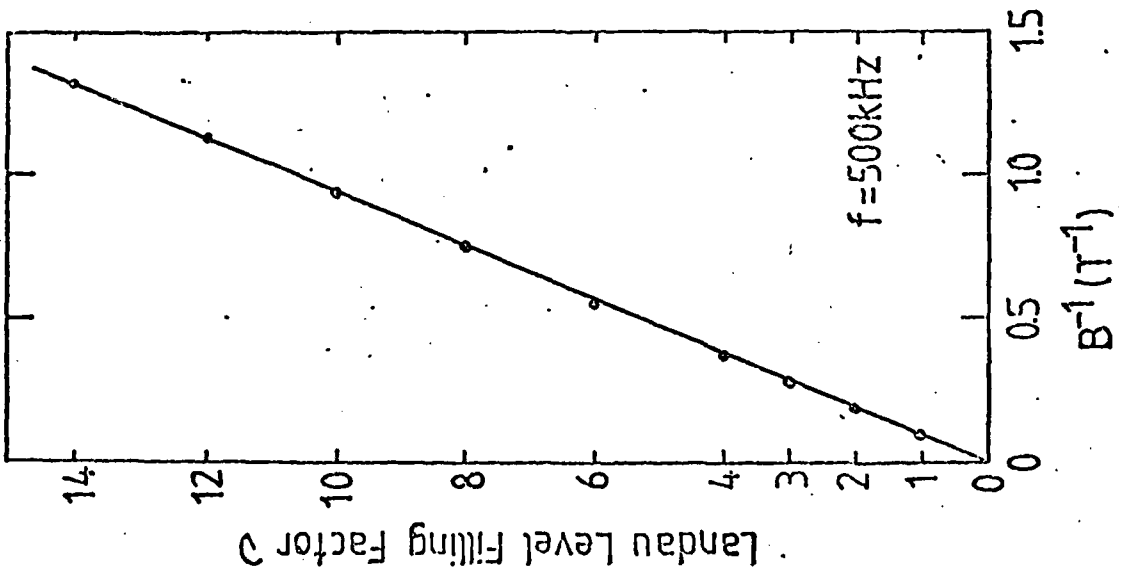


FIG. 5

(a)



(b)

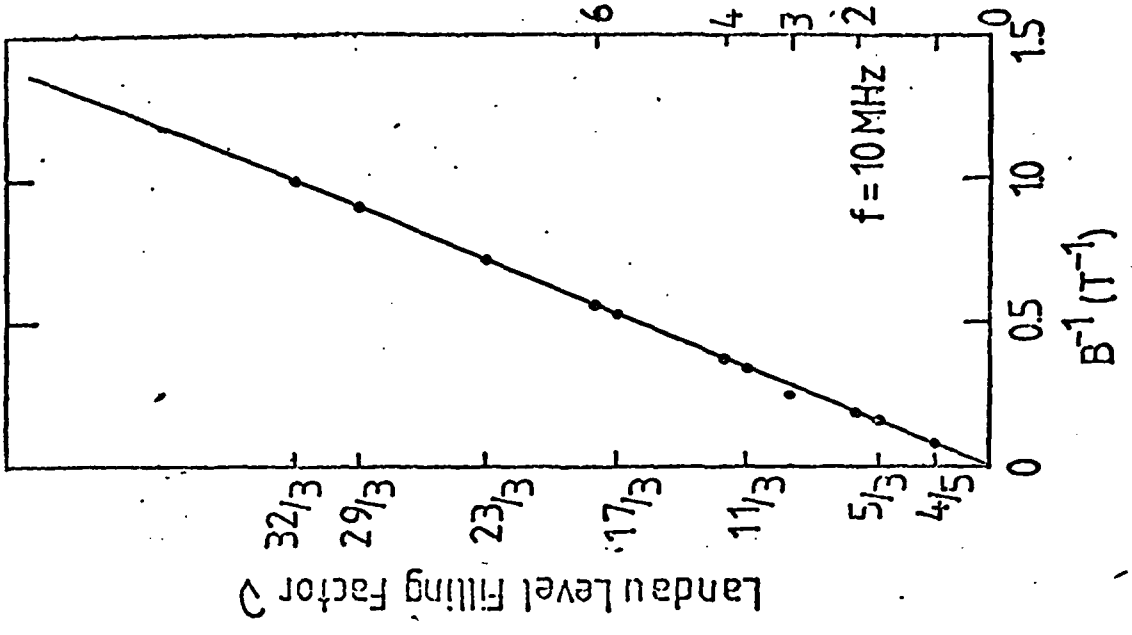
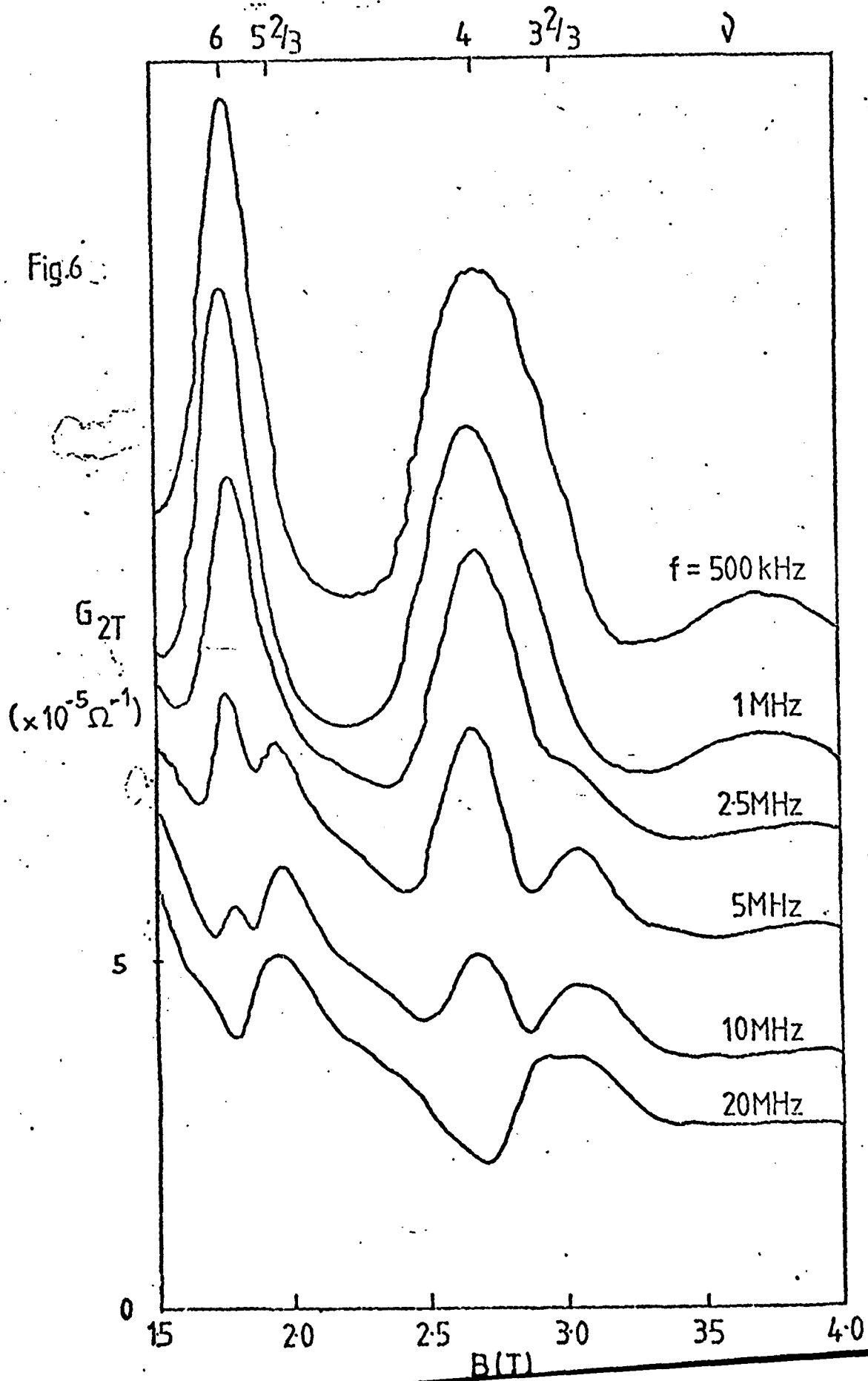


Fig. 6



LETTER TO THE EDITOR

Two-dimensional electron interaction effects in high magnetic fields

R A Davies† and M Pepper‡

Cavendish Laboratory, University of Cambridge,
Madingley Road, Cambridge, CB3 0HE, UK

Received 26 April 1983

Abstract. We have investigated the interaction contributions to the conductivity of silicon inversion layers in the presence of high magnetic fields. When Landau levels are formed, a sign change in the temperature dependence of the resistance has been found. This is not present in the correction to the Hall coefficient; both these effects are in agreement with theoretical predictions.

It is known that the application of a magnetic field to a 2D system separates the weak localisation and interaction corrections to the conductivity (Uren *et al* 1980, 1981, Davies *et al* 1981). The introduction of the cyclotron length, L_c , decreases the length scale determining the magnitude of the localisation correction. When $L_c \ll L_{IN}$ (the inelastic diffusion length) the localisation correction becomes virtually temperature-independent, although negative magnetoresistance is found until $L_c \approx l$ where l is the mean free path for elastic scattering. The condition that $L_c \approx l$ corresponds to

$$\omega\tau \approx 1/k_F l$$

where k_F is the Fermi wavevector, ω is the cyclotron frequency and τ is the mean free time for elastic scattering. The condition for the observation of strong Shubnikov-de Haas oscillations is $\omega\tau \approx 1$ and if $k_F l > 1$ it is clear that the weak localisation is suppressed before the onset of the oscillatory magnetoresistance. The magnetic field also changes the screening properties of the electrons, thus enhancing interaction effects. This is a spin effect whereas the suppression of the localisation is orbital. The theory of interaction effects when the density of states is split into Landau levels has been considered for the conditions $E_F \tau > 1$ and $\omega\tau > 1$ (Houghton *et al* 1982a, b), where E_F is the Fermi energy. The predicted corrections to the unperturbed resistance R^0 and Hall constant R_H are given below:

$$\frac{\Delta R}{R^0} = -R_{\square}^0 \frac{ge^2}{2\pi^2 \hbar} (1 - \omega^2 \tau^2) \ln(T/T_0) \quad (1)$$

$$\frac{\Delta R_H}{R_H^0} = -2R_{\square}^0 \frac{ge^2}{2\pi^2 \hbar} \ln(T/T_0). \quad (2)$$

† Now at GEC Research Laboratories, Hirst Research Centre, Wembley, UK

‡ Also at GEC Research Laboratories, Hirst Research Centre, Wembley, UK.

The square suffix signifies ohms per square, the constant $T_0 = \hbar/2\pi k\tau$ and g is the coupling constant, which in a magnetic field sufficiently strong to lift the spin degeneracy is according to theory (in the notation of Fukuyama 1980) $n_v g_1 - g_3 = \frac{1}{2}$ for $n_v = 2$ and the screening constant $F \approx 1$. More appropriately it should be regarded as an empirical parameter. The unperturbed values of R_{\square}^0 and R_H^0 are

$$R_{\square}^0 = m/2N(E_F) E_F e^2 \tau$$

$$R_H^0 = 1/2N(E_F) E_F e.$$

These results predict a ratio

$$\frac{\Delta R_H/R_H^0}{\Delta R/R^0} = \frac{2}{1 - \omega^2 \tau^2}. \quad (3)$$

For $\omega\tau \ll 1$ this yields the well known result for small fields (Altshuler *et al* 1980, Uren *et al* 1980, 1981, Bishop *et al* 1981). The most noticeable consequence of equation (3) is that due to the behaviour of $\Delta R/R^0$ the ratio changes sign as $\omega\tau$ increases through unity.

We have investigated this prediction for transport in the inversion layer of (100 orientation) Si MOSFETs. The method of measurement has been described before (Uren *et al* 1981), the devices had an aspect ratio of unity with potential and Hall probes located at $\frac{1}{4}$ and $\frac{3}{4}$ of the channel length. This geometry introduces a correction into the relation between the Hall constant and the Hall voltage. Previous work in GaAs-GaAlAs heterojunctions by Paalanen *et al* (1982) established the existence of the logarithmic correction when the magnetic field was sufficiently strong to cause Landau level formation. In the work reported here the corrections in the resistance and Hall effect were measured in the conductivity maxima and minima. When the rate of impurity scattering is low, thermal excitation of electrons causes a temperature dependence of conductivity when E_F is in a density of states minimum. In order to avoid this effect, we used samples in which the mobility was low, resulting in a large broadening of the Landau levels, hence any measured temperature dependence of conductivity was the result of the interaction mechanism. The high degree of impurity scattering necessary was achieved by implantation of boron into the channel region; the mobility was $\sim 2900 \text{ cm}^2 \text{ V}^{-1} \text{ s}^{-1}$. An example of the Shubnikov-de Haas oscillations found with these devices is shown in figure 1.

For low values of magnetic field the Hall constant changed twice as rapidly as the resistance, as has been reported previously (Uren *et al* 1980, 1981, Bishop *et al* 1981).

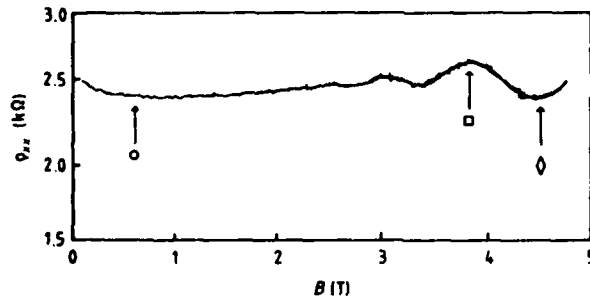


Figure 1. An example of the Shubnikov-de Haas oscillations found with the devices used in this work. The arrows and symbols indicate the values of magnetic field where the temperature dependence was measured, $T = 1.3 \text{ K}$, carrier concentration $10^{12} \text{ electrons/cm}^2$.

The results for higher magnetic fields are shown in figures 2 and 3; it is seen that a logarithmic temperature dependence is found for all cases. The behaviour of the resistance, figure 2, clearly shows that the magnitude of the slope decreases with increasing magnetic field and then changes sign. The sign change is clear at 4.5 T which is slightly smaller than the value of field required to meet the $\omega\tau \approx 1$ condition (4.8 T). This discrepancy may be caused by the field dependence of τ , or possibly a slightly incorrect estimate of τ due to a small error in our estimate of mobility.

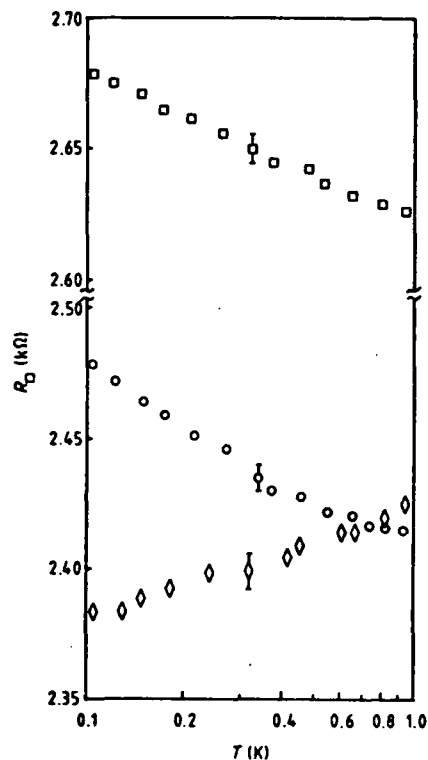


Figure 2. The resistivity as a function of temperature for the values of magnetic field indicated in figure 1. \circ $B = 0.61$ T; \square $B = 3.8$ T; \diamond $B = 4.5$ T.

The predicted temperature dependence of the Hall constant should not change sign but should oscillate as the resistance oscillates with the magnetic field. However, the temperature dependence of the Hall constant increased at 4.5 T, whereas the resistance passed through a minimum. It is possible that this effect is associated with the geometry of the devices not being ideal for measurements of the Hall effect. The percentage change of resistivity, ρ_{xx} , and Hall resistivity, ρ_{xy} , per decade change in temperature are plotted against magnetic field in figure 4.

These corrections do not, of course, have significance for the quantised Hall resistance (von Klitzing *et al* 1980, Pepper and Wakabayashi 1982) as in this experiment ρ_{xx} is zero and, hence, $\Delta\rho_{xy}/\rho_{xy} = 0$.

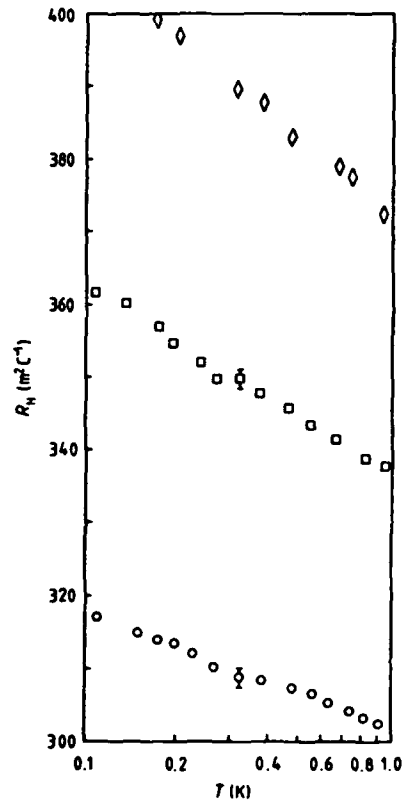


Figure 3. The Hall constant as a function of temperature for the values of magnetic field indicated in figure 1. ○ $B = 0.61$ T, □ $B = 3.8$ T; ◇ $B = 4.5$ T.

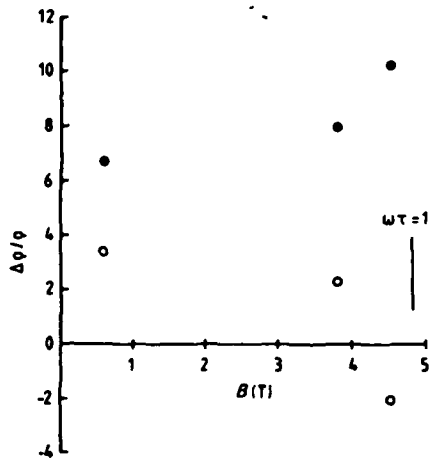


Figure 4. The percentage changes of resistivity (○) and Hall resistivity (●) per decade change of temperature are plotted against magnetic field.

We now consider the interaction effect in the presence of a strong magnetic field applied parallel to the plane of the inversion layer which, of course, does not form Landau levels. It was first shown by Davies *et al* (1981) that the parallel and perpendicular field magnetoresistance is a method of distinguishing between localisation and interaction effects. We present further results on this effect here (figure 5). As is seen, below

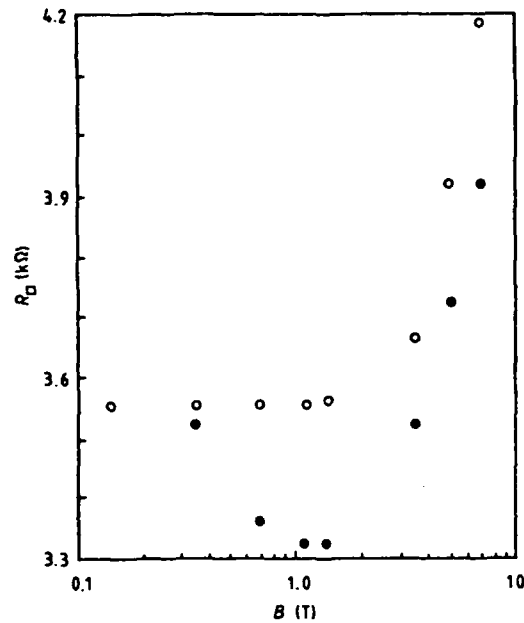


Figure 5. The resistivity is plotted against magnetic field for normal (●) and parallel (○) directions. The carrier concentration is 1.1×10^{12} electrons/cm², temperature is 1.35 K.

0.1 T the resistance is almost field independent but a negative magnetoresistance rapidly develops for the normal field case as localisation is suppressed. For both directions of field the resistance increases above ~ 1 T; as expected this field corresponds to a spin splitting approximately equal to kT ($T = 1.35$ K). The magnitude of the magnetoresistance is larger for a parallel field than for a normal field, as predicted by Kawabata's (1982) calculation in which the effective coupling constant is $g_3 + g_4$ for a parallel field and g_3 for a normal field. Here $g_3 = g_4 = F/2$, and for our experimental conditions $F \approx 1$.

Figure 6 shows the enhancement of the temperature dependence of the resistance in a parallel magnetic field when $g_L \mu_B B > kT$. The values of electron temperature corresponding to electric field are also shown; here we assume that the relationship between electric field and temperature is not affected by the magnetic field. This is reasonable, as it has been verified experimentally (Uren *et al* 1980, Bishop *et al* 1981) that the phonon emission rate is not strongly affected by the field. The results of figure 6 show that a small negative magnetoresistance is present at small fields. This may arise from a sample misalignment as Hall results indicate an angle of 2° between the field and the inversion layer. It is also possible that a mechanism first proposed by Altshuler and Aronov (1981) is responsible. Here, because of the finite thickness of the inversion layer, localisation

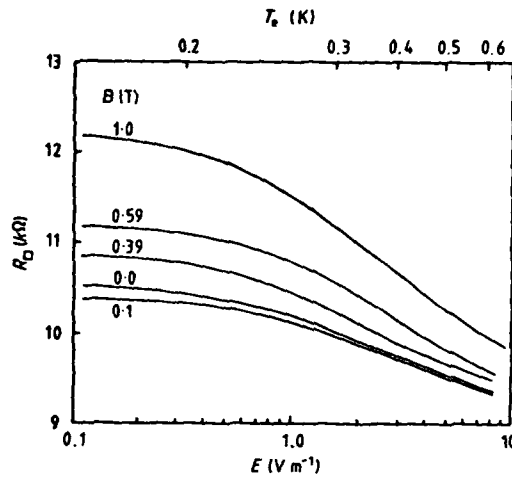


Figure 6. The resistivity as a function of electric field (the electron temperature is the upper scale) for various values of parallel magnetic field.

effects are removed even by a parallel field. Due to the small field misalignment this effect could not be investigated quantitatively.

The magnetoresistance at a constant electron temperature, i.e. constant electric field, can be extracted from figure 6 and other similar data. As the interaction enhancement is a spin effect the magnetoresistance should be a function of $g_L \mu_B B/kT$ only. Figure 7 shows a theoretical curve of parallel field magnetoresistance for a value of coupling constant g of $\frac{1}{2}$. Also shown are experimental points for three electron temperatures. As seen the effective g value appears to increase with increasing temperature. However, it is not clear if this is due to problems with theory or to the presence of the negative magnetoresistance. We note that Dynes (1982) and Bishop *et al* (1982) have found from magnetic field experiments that the value of the coupling constant is bigger than expected and increases with the sample resistivity.

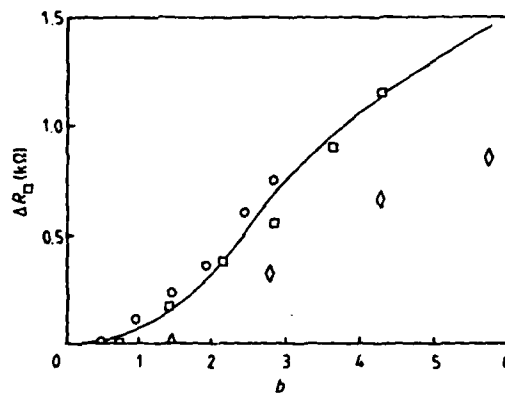


Figure 7. The magnetoresistance from figure 6 plotted against the dimensionless parameter $b = g_L \mu_B B/kT$. The electron temperatures are $\diamond = 0.2$ K, $\square = 0.4$ K and $\circ = 0.6$ K.

We have enjoyed many discussions with Professor Sir Nevill Mott and Dr M Kaveh. R A Davies acknowledges an SERC research studentship. This work was supported by SERC and, in part, by the European Research Office of the US Army.

References

- Altshuler B L and Aronov A G 1981 *JETP Lett.* **33** 499
Altshuler B L, Aronov A G and Lee P A 1980 *Phys. Rev. Lett.* **44** 1288
Bishop D J, Dynes R C and Tsui D C 1982 *Phys. Rev. B* **26** 773
Bishop D J, Tsui D C and Dynes R C 1981 *Phys. Rev. Lett.* **46** 360
Davies R A, Uren M J and Pepper M 1981 *J. Phys. C: Solid State Phys.* **15** L371
Dynes R C 1982 *Surf. Sci.* **113** 510
Fukuyama H 1980 *J. Phys. Soc. Japan* **48** 2169
Houghton A, Senna J R and Ying S C 1982a *Phys. Rev.* **B25** 2169
— 1982b *Phys. Rev.* **B25** 6468
Kawabata A 1982 *Surface Sci.* **113** 527
von Klitzing K, Dorda G and Pepper M 1980 *Phys. Rev. Lett.* **43** 494
Paalanen M A, Tsui D C and Gossard A C 1982 *Phys. Rev. B* **25** 5566
Pepper M and Wakabayashi J 1982 *J. Phys. C: Solid State Phys.* **15** L861
Uren M J, Davies R A, Kaveh M and Pepper M 1981 *J. Phys. C: Solid State Phys.* **14** 5737
Uren M J, Davies R A and Pepper M 1980 *J. Phys. C: Solid State Phys.* **13** L985

LETTER TO THE EDITOR

Non-metallic transport in silicon inversion layers and the Hall effect

R A Davies†‡ and M Peppert§

† Cavendish Laboratory, University of Cambridge, Madingley Road, Cambridge CB3 0HE, UK

§ GEC Research Laboratories, Hirst Research Centre, Wembley, Middlesex, UK

Received 10 February 1983

Abstract. We present results on the Hall effect in the Si inversion layer in the regime where the temperature dependence of the conductivity is due to corrections arising from the electron-electron interaction. We find that the temperature dependence of the Hall coefficient is independent of the magnitude of the magnetic field which does, however, have a pronounced effect on the temperature dependence of the conductivity. This is not explained by present theories, and suggests that whereas the effects of screening on the conductivity are well understood this is not the case with the Hall effect.

Recent advances in the understanding of transport in two dimensions have shown that, even in the weak-scattering limit, deviations from metallic conduction will occur at low temperatures. These deviations arise from two distinct sources: the so-called localisation and interaction effects.

The localisation effect is a reduction in the diffusion coefficient as a result of back-scattering and quantum interference. Perturbation calculations by Gorkov *et al* (1979) and Abrahams and Ramakrishnan (1980) have shown that, to first order, conductivity is

$$\sigma(T) = \sigma_0 + \frac{n_v \alpha p e^2}{\pi^2 \hbar} \ln(T/T_0). \quad (1)$$

σ_0 is the unperturbed conductivity, n_v is the valley degeneracy, α is a constant of order $1/n_v$, p is the index of the inelastic scattering rate, $\tau_{in} \propto T^{-p}$, T is the temperature and T_0 is a constant. An interpretation proposed by Anderson *et al* (1979) has been used to incorporate finite temperatures into the perturbation results.

It has been shown by Hikami *et al* (1980) and Altshuler *et al* (1980b) that the logarithmic correction should be suppressed by classically small magnetic fields, negative magnetoresistance accompanying this.

The second term, the interaction effect, is the result of interference between impurity scattering and the electron-electron interaction. Altshuler *et al* (1980a) and Fukuyama (1980a) have shown that a logarithmic correction is also expected from this mechanism:

$$\Delta\sigma = (ge^2/2\pi^2\hbar) \ln(T/T_1) \quad (2)$$

where T_1 is a constant and g is a 'coupling constant'.

‡ Now at the GEC Research Laboratories, Hirst Research Centre, Wembley, Middlesex, UK.

There is some controversy over the exact value of g (Lee and Ramakrishnan 1982, H Fukuyama, private communication), but it is generally agreed that in the case of (100) silicon inversion layers it should be small because of the short screening length.

Experimental work by Uren *et al* (1980) showed that this term is enhanced by a magnetic field. Later theoretical work by Kawabata (1982) and Lee and Ramakrishnan (1982) showed that this could be explained by including the effect of spin splitting in the calculations. In a large field such that $g_L \mu_B B > k_B T$ (g_L is the Landé factor, μ_B is the Bohr magneton and B is the magnetic field) certain terms are suppressed, so the value of g in equation (2) is enhanced.

The localisation and interaction terms are additive to first order (Kaveh and Mott 1981, Houghton *et al* 1982).

We now turn to the subject of this Letter: the Hall effect.

Corrections to the Hall effect from localisation have been considered by Fukuyama (1980b) and Altshuler *et al* (1980b). They have shown that there should be no correction to first order in the Hall constant R_H , i.e.

$$\Delta R_H = 0. \quad (3)$$

The corresponding result from the interaction effect has been calculated by Altshuler *et al* (1980a). They have shown that $\Delta \sigma_{xy} = 0$, so that

$$\Delta R_H / R_H = 2\Delta R / R. \quad (4)$$

It should be noted that certain terms (g_2 and g_4 in Fukuyama's notation) have not been included in this calculation. The contribution of these terms to the conductivity has been shown by Fukuyama (1981a) to be suppressed by small magnetic fields.

Fukuyama (1980c, d) has considered the effect of valley degeneracy on all these results and has shown that they are not significantly changed.

Experimental work on the Hall effect by Uren *et al* (1980, 1981) and Bishop *et al* (1981) have confirmed equation (4). These results were for 'large' magnetic fields, where localisation effects are suppressed and interaction effects enhanced.

Uren *et al* (1981) and Fukuyama (1982) give comprehensive discussions of all these effects; here we concentrate on the Hall effect in small magnetic fields. This is an area of great interest on which very little has been published.

The measurements were performed on (100) n -channel silicon MOSFETS, size $250 \times 250 \mu\text{m}$, with two pairs of contacts at $\frac{1}{4}$ and $\frac{3}{4}$ along the side. An implant of boron into the channel region was used to control the mobility. Conventional low-frequency AC measuring methods were used, with phase sensitive detection; a four-terminal resistance or Hall resistance could be measured by using appropriate pairs of contacts.

Low temperatures were obtained using two cryostats: one was a dilution refrigerator covering the range 0.1 to 1 K with magnetic fields of up to 5 T and the other was a ^3He evaporation cryostat covering the range 0.5 to 5 K with fields of up to 0.2 T.

An extensive discussion of experimental techniques has been given elsewhere (Uren *et al* 1981); a few pertinent points are summarised here.

Electric fields in the range 0.1 to 1 V m^{-1} were used, depending on the temperature, to ensure that no electron heating occurred.

In measurements of the Hall effect, results for both directions of magnetic field were averaged. This was necessary as, when very small Hall voltages were measured, an error existed due to macroscopic inhomogeneities giving rise to non-uniform current paths. The measuring method gave a resolution of better than 0.1% but absolute accuracy was

much less; about 4%. This should be borne in mind when comparing results for different magnetic fields.

Figure 1 shows the results of measurements of the temperature dependence of resistance in magnetic fields of 0, 0.1 and 0.61 T. In the absence of a magnetic field the temperature dependence is due mainly to localisation, and can be described by equation (1) with $n_v a p \approx 0.7$. In the small field of 0.1 T no temperature dependence is observed.

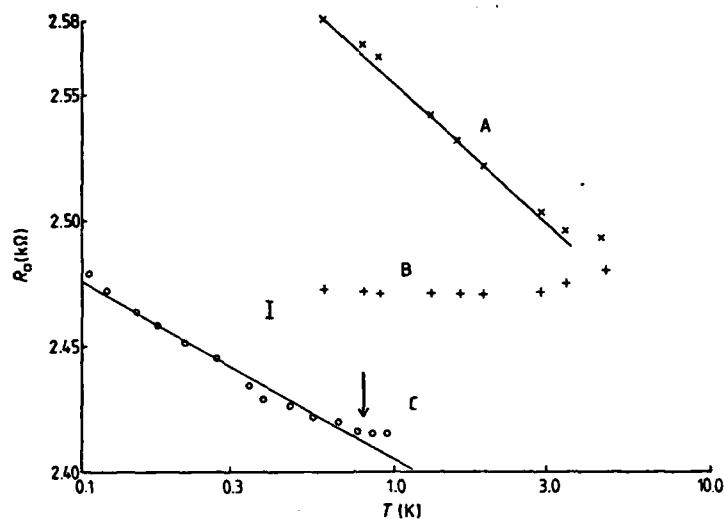


Figure 1. The effect of a magnetic field on the temperature dependence of resistance of the device used for the Hall measurements in figure 2. The transition is clear from localisation behaviour (A) at zero magnetic field which is suppressed in (B) with $B = 0.1$ T and (C) interaction behaviour with $B = 0.61$ T. The error in the resistance is indicated and the arrow illustrates the temperature at which $kT = g_L \mu_L B$ and, as expected, the interaction effect vanishes with increasing temperature. The carrier concentration is 10^{16} electrons/cm².

This is expected from the work of Hikami *et al* (1980) and Altshuler *et al* (1980b). Above 3 K the resistance starts to rise with temperature. This is believed to be the result of a temperature dependence in the elastic scattering rate (Stern 1980), and will not be discussed further. When the field is increased to 0.61 T the logarithmic temperature dependence reappears. This is the interaction effect which is enhanced when the spin degeneracy is lifted. The line is the theoretical curve (equation (2)) with the coupling constant $g = \frac{1}{2}$. Above 0.6 K the temperature dependence decreases. This is also expected as $g_L \mu_B B = k_B T$ at 0.8 K, so that the spin degeneracy is restored above this temperature.

The corresponding results for the Hall effect are shown in figure 2, for fields of 0.1 and 0.61 T. Taking first the results for 0.61 T, where interactions are known to dominate, the temperature dependence in the Hall constant is exactly as expected; the line is the theoretical curve $R_H/R_H = 2R/R$, with R/R taken from the corresponding result in figure 1. This ratio of two has been observed over a wide range of conditions (where interactions dominate) by Uren *et al* (1980, 1981). It should be noted that the temperature dependence of R_H continues beyond 0.6 K, which is not consistent with the theoretical prediction.

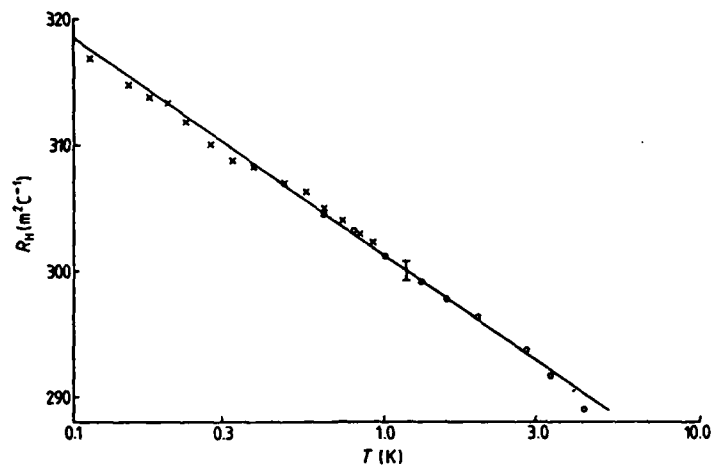


Figure 2. The temperature dependence of the Hall constant for the same device and conditions as figure 1. The points \times were taken at a magnetic field of 0.61 T and \circ were at 0.1 T. As the magnetic field is only known to 5% it was not possible to obtain the absolute value of the Hall constant to the same accuracy as the measurement of the change. In order to display the field independence of the rate of change of R_H the 1 K reading at 0.1 T was normalised to the same value as the 0.61 T result, and the other 0.1 T readings were all multiplied by the normalisation factor. Due to the geometry of the device the absolute value of R_H is approximately a factor of 2 too small. The value of $\Delta R_H/R_H$ is unaffected by the geometry.

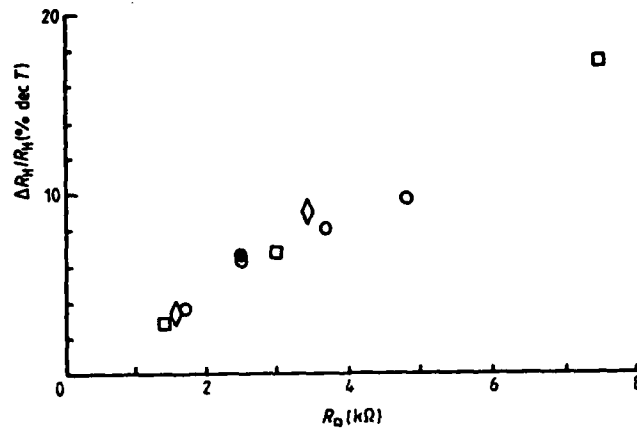


Figure 3. The percentage change in the Hall constant, per decade change in temperature, plotted against resistivity (sheet resistance) R_{\square} for three devices. The threshold voltages and mobilities μ of these devices were adjusted by ion implantation. The values of μ ($\text{m}^2 \text{V}^{-1} \text{s}^{-1}$) and magnetic field B (T) were as follows: \square $B = 0.1$ T, $\mu = 0.39$; \circ $B = 0.1$ T, $\mu = 0.29$. \bullet was the same device as \circ but $B = 0.61$ T; \diamond $B = 0.1$ T, $\mu = 0.23$. As seen the results \circ and \bullet are identical for the same value of R_{\square} and are independent of magnetic field.

The relation $\Delta R_H/R_H \propto R_{\square}$ is characteristic of interactions, following from $\Delta R_{\square} \propto R_{\square}^2 \Delta \sigma$ and $\Delta R_H/R_H \propto \Delta R_{\square}/R_{\square}$.

Much more interesting are the results for the 0.1 T magnetic field. It can be seen that a temperature dependence similar to that in the 0.61 T field is present in the Hall effect while *no* temperature dependence is visible in the resistance. This result was totally unexpected and so the Hall effect in small fields was studied in greater detail. The results are summarised in figure 3. Here the percentage change in the Hall constant per decade change in temperature is plotted against resistivity, for a field of 0.1 T. Also shown is the corresponding result, taken from figure 2, for a 0.61 T field. It lies almost on top of the result for 0.1 T, while the ratio $g_L \mu_B B / k_B T$ is in the range 1 to 8 for 0.61 T and 0.02 to 0.25 for 0.1 T. This suggests that the same mechanism is responsible in each case.

The relationship $\Delta R_H / R_H \propto R$ is characteristic of interactions, and is implicit in the experimental results of Uren *et al* (1980), for large fields. Further evidence for the same mechanism being responsible in both cases comes from the points in figure 2 for 0.61 T; the temperature dependence of the Hall constant does not change with $g_L \mu_B B \sim k_B T$ while the temperature dependence of the resistance does.

Some measurements have also been made at lower magnetic fields where the temperature dependence from localisation appears in the resistance. Figure 4 shows plots of Hall voltage against magnetic field for two temperatures; an offset of $2 \mu\text{V}$ has been subtracted. The corresponding plots of the magnetoresistance are shown in figure 5. The Hall voltage measurements suggest that the temperature dependence of the Hall constant persists to fields below 0.01 T and is not greatly influenced by the appearance of weak localisation. Over this range of magnetic field the temperature dependence of resistance changes noticeably.

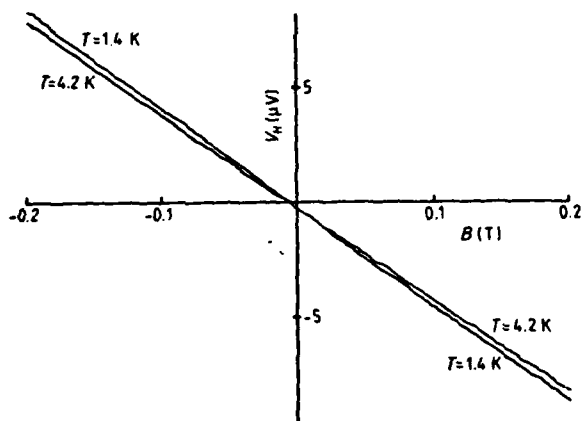


Figure 4. Here we illustrate the behaviour of the Hall voltage as a function of magnetic field for two temperatures 4.2 K and 1.4 K. The device had a carrier concentration of 7×10^{15} electrons/m² and a constant current of 10^{-7} A was passed. As seen, the Hall voltage V_H increases linearly with B and shows a temperature dependence down to the lowest fields. The effect is present despite the presence of weak localisation which is illustrated in figure 5.

All these results suggest that there is a correction to the Hall constant from interactions but not from weak localisation. The magnitude of this correction is the same over a wide range of magnetic fields while the corresponding correction to the resistivity varies by different amounts. At present no explanation of this is available but it should be noted that the contributions of g_2 and g_4 processes to the Hall effect have not yet been calculated.

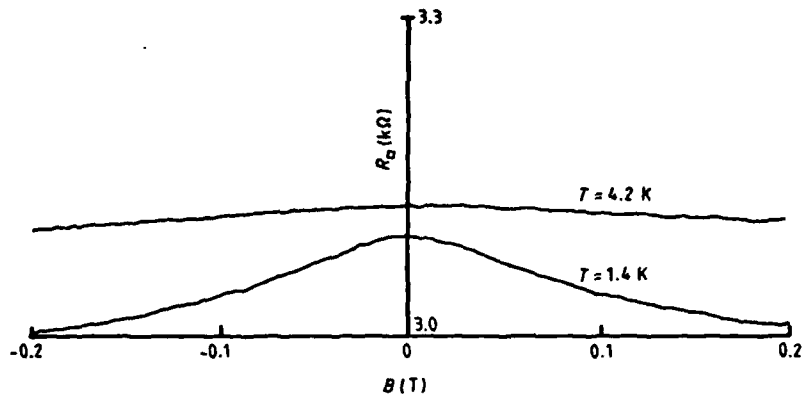


Figure 5. The relation between the magnetic field and resistivity corresponding to figure 4 is displayed. It is seen that the weak localisation is substantially suppressed by a field of 0.2 T at 1.4 K although not at 4.2 K where the inelastic diffusion length is short. These differences in the suppression of the weak localisation do not affect the behaviour of the Hall constant, as illustrated in figure 4.

Experiments on silicon inversion layers by Dynes (1982) have produced very different results. He has found that the ratio $\Delta R_H/R_H : \Delta R/R$ falls towards zero at small magnetic fields but has not reported the actual temperature dependence. Experiments by Poole *et al* (1981) on GaAlAs heterostructures are in better agreement with our results. They have found a temperature dependence, but no magnetic field dependence, in the Hall constant under similar experimental conditions. In that system interactions are always present because of the longer screening length.

Finally, we consider the physical significance of our finding that $\Delta R_H/R_H$ is independent of magnetic field, and, hence, is independent of the magnitude of the temperature dependence of the interaction contribution to the resistance. As we have found that there is no localisation contribution to the Hall constant, it is clear that, in the notation of Fukuyama (1980a), the term $(n_v g_1 - 2g_3)$, which becomes $(n_v g_1 - g_3)$ in high magnetic fields, does not determine the temperature dependence of the Hall constant. If we inspect the various terms contributing to the interaction process, then the requirement that $\Delta R_H/R_H$ is independent of B implies that there is a correction in the Hall conductance, σ_{xy} , given by

$$\sigma_{xy} = 2\omega\tau\Delta\sigma_3.$$

Here ω is the cyclotron frequency, τ is the elastic scattering time and $\Delta\sigma_3$ is the contribution to the conductivity given by the antiparallel spin Hartree term

$$\Delta\sigma_3 = \frac{e^2}{2\pi^2\hbar} g_3 (G(b) - \ln(T/T_0)).$$

Here g_3 is the coupling constant, and the function $G(b)$ must be evaluated numerically. The limiting forms of $G(b)$ are given by Kawabata (1982) as

$$G(b) = -0.09/4b^2 \quad (\text{for } b \ll 1)$$

$$G(b) = -\ln b - 0.258 + \pi^2/3b^2$$

$$b = g_L \mu_B / kT.$$

At high fields $\Delta\sigma_z$ becomes zero and, as predicted by Fukuyama (1980b) and Altshuler (1980b), $\Delta\sigma_{xy} = 0$. However, at low fields this term dominates as, in the inversion layer, screening effects reduce the magnitude of the interaction effect, and $\Delta\sigma_{xx} = 0$. Thus the temperature dependence of $\Delta R_H/R_H$ is unaffected by the magnitude of the magnetic field and the modification of the net coupling constant.

In conclusion it appears that whereas the understanding of screening appears adequate for explaining the effects of the electron-electron interaction on the conductivity, this is clearly not the case for the Hall effect.

We have enjoyed many stimulating discussions with Professor Sir Nevill Mott and Dr M Kaveh. This work was supported by SERC and, in part, by the European Research Office of the US Army. R A Davies acknowledges an SERC Research Studentship.

References

- Abrahams E and Ramakrishnan T V 1980 *J. Non. Cryst. Solids* **35** 15
Altshuler B L, Aronov A G and Lee P A 1980a *Phys. Rev. Lett.* **44** 1288
Altshuler B L, Khmel'nitzkii D E, Larkin A I and Lee P A 1980b *Phys. Rev.* **B22** 5142
Anderson P W, Abrahams E and Ramakrishnan T V 1979 *Phys. Rev. Lett.* **43** 718
Bishop D J, Tsui D C and Dynes R C 1981 *Phys. Rev. Lett.* **46** 360
Dynes R C 1982 *Surface Sci.* **113** 510
Fukuyama H 1980a *J. Phys. Soc. Japan* **48** 510
— 1980b *J. Phys. Soc. Japan* **49** 2169
— 1980c *J. Phys. Soc. Japan* **49** 644
— 1980d *J. Phys. Soc. Japan* **49** 649
— 1981a *J. Phys. Soc. Japan* **50** 3407
— 1981b *J. Phys. Soc. Japan* **50** 3562
— 1982 *J. Phys. Soc. Japan* **113** 489
Gorkov L P, Larkin A I and Khmel'nitzkii D E 1979 *JETP Lett.* **30** 248
Hikami S, Larkin A E and Nagaoka Y 1980 *Prog. Theor. Phys.* **63** 707
Houghton A, Senna J R and Ying S C 1982 *Phys. Rev.* **B25** 2169
Kaveh M and Mott N F 1981 *J. Phys. C: Solid State Phys.* **14** L183
Kawabata A 1982 *Surface Sci.* **113** 527
Lee P A and Ramakrishnan T V 1982 *Phys. Rev.* **B26** 4009
Poole D A, Pepper M and Glew R W 1981 *J. Phys. C: Solid State Phys.* **14** L995
Stern F 1980 *Phys. Rev. Lett.* **44** 1469
Uren M J, Davies R A, Kaveh M and Pepper M 1981 *J. Phys. C: Solid State Phys.* **14** 5737
Uren M J, Davies R A and Pepper M 1980 *J. Phys. C: Solid State Phys.* **13** L985

LETTER TO THE EDITOR

Electron-electron scattering in silicon inversion layers

R A Davies^{†‡} and M Peppert^{‡§}

[†] Cavendish Laboratory, University of Cambridge, Madingley Road,
Cambridge CB3 0HE, UK

[§] GEC Research Laboratories, Hirst Research Centre, Wembley, Middlesex, UK

Received 31 January 1983

Abstract. We present the results of an investigation of the rate of electron-electron scattering in the two-dimensional electron gas of the Si inversion layer. The electron-electron scattering rate was extracted by analysis of the negative magnetoresistance in the regime of weak localisation when $k_F l > 1$, where k_F is the Fermi wavevector and l is the mean free path for elastic scattering. The results showed that over a wide range of $k_F l$, carrier concentration and electron mobility the scattering rate was given by two processes which were additive. The first was the normal T^2 (Landau-Baber) law and the second was the T law expected when the effects of disorder are considered.

There was no evidence for the recently proposed $T \ln T$ law.

Recent advances in the understanding of localisation have shown that at low temperature deviations from metallic conduction occur. The form of the deviation has been calculated for two dimensions (Abrahams *et al* 1979, Gorkov *et al* 1979, Kaveh and Mott 1981 and others) as

$$\Delta\sigma = (n_v \alpha e^2 / 2\pi^2 \hbar) \ln(\tau_i / \tau)$$

where n_v is the valley degeneracy, α is a constant of order one, τ_i is the inelastic scattering time and τ is the elastic, impurity, scattering time.

The magnetoresistance associated with this has been considered by Hikami *et al* (1980) and Altshuler *et al* (1980). They derived the expression

$$\Delta\sigma = (n_v \alpha e^2 / 2\pi^2 \hbar) [\psi(\frac{1}{2} + 1/a\tau_i) - \psi(\frac{1}{2} + 1/a\tau)]$$

where ψ is the digamma function (Abramowitz and Stegun 1970), B is the magnetic field, D is the diffusivity of the electrons and $a = 4eBD/\hbar$. The constant α was originally treated as an empirical parameter to improve the agreement with experimental results. Fukuyama (1980a) has shown that it is the result of intervalley scattering; at low temperatures $n_v \alpha = 1$ is expected with $\alpha = 1$ at high temperatures.

By fitting the theoretical expression to the experimental results, using α and τ_i as parameters, the inelastic scattering time is determined. This has been done by many groups, initially Kawaguchi and Kawaji (1980) and Uren *et al* (1981a, b). It has been established that electron-electron scattering is the dominant scattering mechanism and that the T^2 law is modified in the presence of impurity scattering. As has been shown by

[‡] Now at GEC Research Laboratories, Hirst Research Centre, Wembley, Middlesex, UK.

Altshuler *et al* (1980a, b) and Fukuyama (1980b) the interference between impurity scattering and Coulomb interactions also gives deviations from metallic conduction. These effects are small in inversion layers (Uren *et al* 1981a, b); Fukuyama (1981) has shown that they can be included by modifying slightly the value of α . More extensive discussions of deviations from metallic behaviour can be found in the papers by Uren *et al* (1981a, b) and Fukuyama (1982).

Here the results of a systematic study of inelastic (electron-electron) scattering are presented. First the available theories of electron-electron scattering will be discussed.

At low temperatures this is the dominant mechanism of inelastic scattering (Ashcroft and Mermin 1976). The normal form is Landau-Baber scattering, where the mean free time τ_i varies as

$$1/\tau_i = a(kT)^2/\hbar E_F$$

where a is a constant of order one.

Schmid (1974) and Altshuler and Aronov (1979) have considered the effect of impurity scattering on τ_i . They found that collisions with small momentum transfer, where $\hbar Dq^2 \sim kT$, also make a significant contribution to the scattering rate. In three dimensions this gives an extra term $1/\tau_i \propto T^{3/2}$. Uren *et al* (1981a) found that the corresponding result in two dimensions is

$$1/\tau_i = bkT/E_F \tau$$

where b is a constant of order one. The 'normal' and 'anomalous' rates should be added.

Abrahams *et al* (1981) have performed a similar calculation with a dynamically screened interaction. They found a rate

$$1/\tau_i = (2kT/\hbar k_F l) \ln(T_1/T)$$

with

$$kT_1 = \left(\frac{\hbar^6 K^4}{m^2} \right) \left(\frac{E_F \tau}{\hbar} \right) \left(\frac{4\pi\epsilon_0 \epsilon}{e^2} \right)^2$$

where K is the inverse of the screening length. For (100) silicon

$$T_1 = 3.6 \times 10^6 (k_F l)^3$$

where l is the elastic mean free path.

As T_1 is always large compared with T this logarithmic term can be treated as a constant so that

$$\frac{1}{\tau_i} \left(\frac{k \ln T_1}{E_F \tau} \right) T.$$

The total scattering rate can then be written

$$\frac{1}{\tau_i} = A_1 T + A_2 T^2.$$

It is not obvious from the work of Abrahams *et al* whether the two scattering rates are additive in their calculation, but it should be valid as a first approximation.

The devices used in this work were n-channel silicon MOSFETs, grown on the (100) surface. Table 1 gives the important parameters of those used.

Table 1. Device characteristics. Substrate doping 7.4×10^{20} acceptors/m³.

Device	Oxide thickness d_{ox} (nm)	Implant atoms (m ⁻²)	Threshold voltage V_t (V)	Mobility μ (m ² V ⁻¹ s ⁻¹)
CC8116/1	96	8.3×10^{15}	2.7	0.65
CC8116/2	96	2.2×10^{16}	5.4	0.39
CC8116/3	96	3.6×10^{16}	6.8	0.29
CC8116/4	96	4.9×10^{16}	7.9	0.23
JH1/15	80	—	0.2	0.28

The CC8116 devices had a $250 \times 250 \mu\text{m}$ square channel with pairs of potential probes $\frac{1}{3}$ and $\frac{2}{3}$ along the side. They were manufactured using silicon gate technology; the gate was formed from polycrystalline silicon and an implant of boron into the surface region was used to control the mobility.

The JH1 device was made using conventional aluminium gate methods. The channel length was 2 mm and the width $400 \mu\text{m}$. Pairs of potential probes were positioned $\frac{1}{3}$ and $\frac{2}{3}$ along the side.

The sample resistances were measured by low-frequency AC methods with phase sensitive detection; a constant current was passed along the channel and the voltage between adjacent potential probes measured. To prevent electron heating the voltage drop was always below $100 \mu\text{V}$, corresponding to electric fields below 1 V m^{-1} .

Measurements were made over the temperature range of 0.5 to 5 K. This was provided by a ³He evaporation cryostat and a calibrated germanium thermometer was used to measure the temperature. A small superconducting solenoid was used to produce fields of up to 0.2 T. This was energised by an industrial power amplifier so that fields of either direction could be produced.

Figure 1 shows some typical results. The resistance is plotted against magnetic field

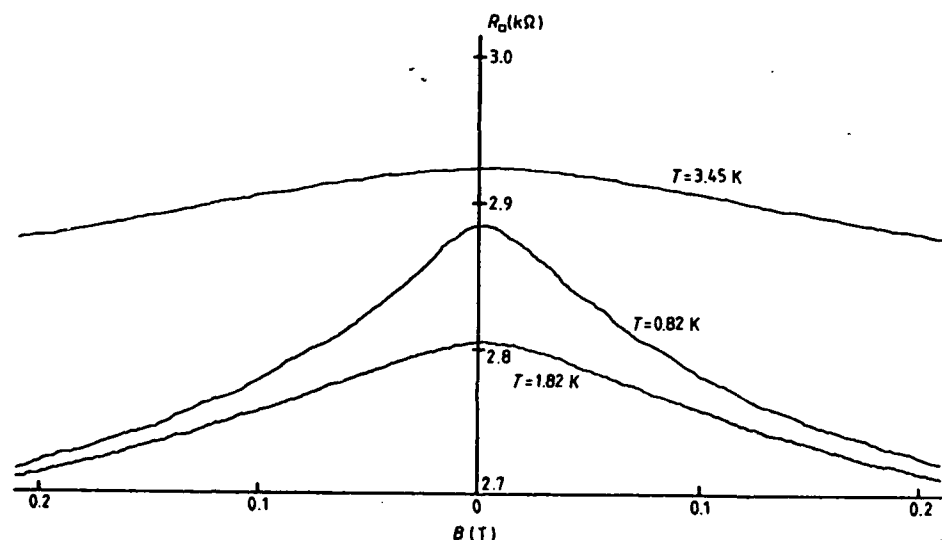


Figure 1. The variation for the JH1/15 of device resistance R_D , in ohms per square, as a function of magnetic field B in Tesla for the indicated temperatures. $n_{inv} = 1.0 \times 10^{16} \text{ m}^{-2}$.

for three temperatures. This was done for a number of temperatures and carrier concentrations for each device. It will be noticed that the temperature dependence at zero field is not monotonic, but passes through a minimum. This is the result of a temperature dependence in the elastic scattering and has been discussed by Stern (1980).

The form the magnetoresistance plots should follow has been given. An approximate version of this was in fact used:

$$\Delta R_{\square} = R_{\square}(B=0) \frac{n_v \alpha e^2}{2\pi^2 \hbar} [\ln(\hbar/4eBD\tau_i) - \psi(\frac{1}{2} + \hbar/4eBD\tau_i)]$$

$$D = 2\pi^2 \hbar / n_v \alpha e^2 R_{\square}(B=0) \quad (n_v = 2).$$

Curves of this form were fitted using τ_i and α as variable parameters. This was done by trial and error, plotting the theoretical curve with trial values, comparing with the results and adjusting the parameters until a good fit was obtained.

The functional form given is not exact, but differs from the true form only at large magnetic fields, which were not reached. A very small systematic error is also introduced by the expression used for the diffusion coefficient D .

Figure 2 shows an example of this fitting procedure; the crosses show experimental points taken from figure 1 and averaged over both field directions; the lines are the fitted curves for the values of α and τ_i shown.

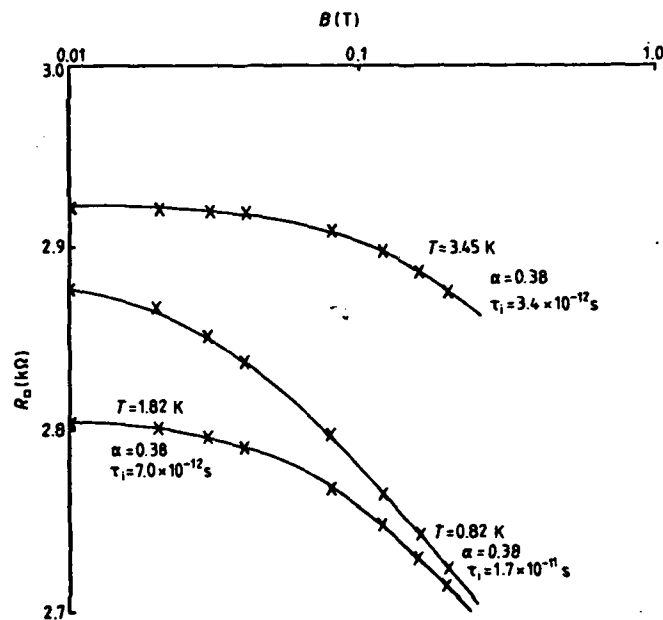


Figure 2. Examples of the fitting between theory and experiment for the JH1/15 device. The values of temperature (T), α and τ_i are shown. $n_{mv} = 1.0 \times 10^{13} \text{ m}^{-2}$.

The parameter α should be $\frac{1}{2}$ according to theoretical calculations. In fact it is slightly less. Fukuyama (1981) has suggested that this reduction is the result of Coulomb interactions. The experimental behaviour of α is discussed in some detail by Kawaguchi and Kawaji (1982) and will not be considered further here. The temperature dependence of

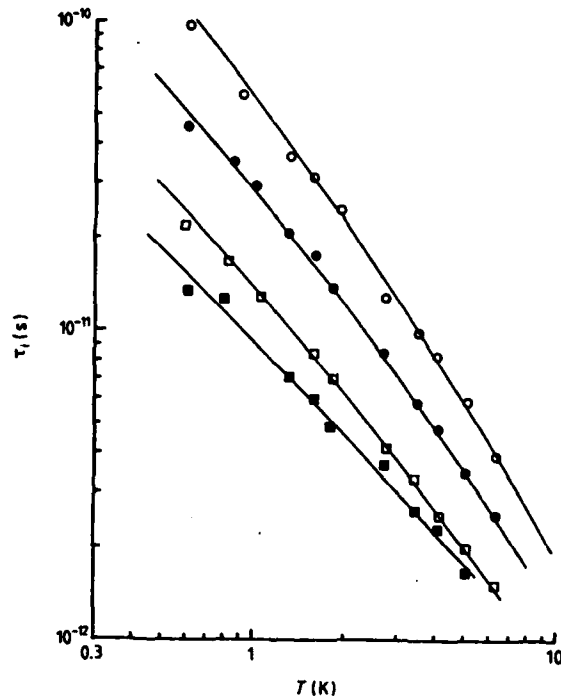


Figure 3. The inelastic scattering time τ_i , in seconds, is plotted against temperature for a JH1/15 device. The lines are fitted curves $1/\tau_i = A_1 T + A_2 T^2$; further details are given in table 2.

the inelastic scattering time is of much greater interest. In figure 3 this is shown for four different carrier concentrations; parameters are given in table 2. Similar results have been reported for inversion layers by Kawaguchi and Kawaji (1980, 1982), Uren *et al* (1981a, b), Wheeler (1981) and Bishop *et al* (1982), for GaAs-GaAlAs heterostructures by Poole *et al* (1981) and for InP inversion layers (Poole *et al* 1982). The results have conventionally been fitted by a power law $\tau_i \propto T^{-p}$, where p varies between 1 and 2, showing that electron-electron scattering, with the extra T term from impurity scattering, is responsible.

Instead of fitting a power law an interpretation first proposed by Uren *et al* (1981a, b) was adopted; the scattering rate was assumed to be the sum of T and T^2 contributions.

Table 2. Parameters for figure 3.

Symbol	n_{inv} (10^{16} m^{-2})	k_{Fl}	A_1 ($10^{10} \text{ K}^{-1} \text{ s}^{-1}$)	A_2 ($10^{10} \text{ K}^{-2} \text{ s}^{-1}$)
○	3.6	22	1.3	0.43
●	1.9	11	3.0	0.51
□	1.0	4.2	6.5	0.7
■	0.63	1.05	13.0	†

† The fitted value was smaller than the experimental error.

A curve of the form

$$\frac{1}{\tau_i} = A_1 T + A_2 T^2$$

was fitted to the data by the method of least squares with A_1 and A_2 as variables. The fitted curves are shown in figure 3 and the A_1 and A_2 values are given in table 2. Fits of this kind were carried out for all the devices to allow comparison of the constants A_1 and A_2 with the calculated values.

The T^2 term comes from conventional Landau-Baber scattering. Using the constant density of states: $N(E) = 2mn_v/2\pi\hbar^2$, where $n_v = 2$; the expected prefactor can be written

$$A = 2ak^2m/\pi\hbar^3n_{inv}$$

where n_{inv} is the inversion layer carrier concentration. (Abrahams *et al* (1981) give a different expression $1/\tau_i = V_F K (kT/\hbar E_F)^2$ but this should be correct only in the limit of poor screening which does not apply here.)

Figure 4 shows the fitted values of A plotted against the carrier density. Also shown is the theoretical curve for $a = 5$. Good agreement is found over a wide range of conditions, confirming that the T^2 term arises from Landau-Baber scattering.

The T term is the 'anomalous' part. According to the theory of Abrahams *et al* (1981) the prefactor should be

$$A_1 = \frac{2k}{\hbar k_F l} \ln[3.6 \times 10^6 (k_F l)^3].$$

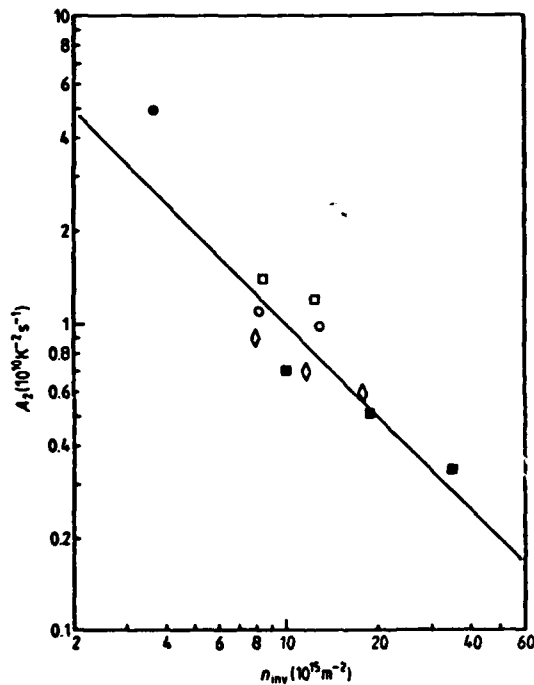


Figure 4. The obtained values of A_2 are plotted as a function of carrier concentration. The theoretical line for $A_2 = 5k_b^2/\hbar E_F$ is shown; the devices are ● CC8116/1, □ CC8116/2, ○ CC8116/3, ◇ CC8116/4, ■ JH1/15.

With static screening, as calculated by Uren *et al* (1981a, b), the logarithmic term is absent, so that

$$A_1 = 2k/\hbar k_{F1}.$$

Both are functions of $k_{F1}l$ only. $k_{F1}l$ is given by

$$\sigma = n_v e^2 k_{F1} / 2\pi\hbar.$$

In figure 5 experimental values of A_1 are plotted against $k_{F1}l$ together with the theoretical curves for dynamic screening (upper line) and static screening (lower line). As can be seen, over a wide range of conditions, the experimental values fit the theory which assumes only static screening, the more sophisticated theory being in error by a large factor.

Bishop *et al* (1982) have presented similar results but have reached very different conclusions. Their scattering times are similar but they have claimed agreement with the calculation assuming dynamic screening. They have, however, ignored the contribution of the T^2 term. In this context it should be noted that their plots of τ_i against $1/T$, which are supposed to show the T dependence, in fact, have a significant non-zero intercept which they have not explained and indicates that their analysis is incorrect.

Finally, after this work was completed further theoretical advances have been made. Fukuyama (private communication) has indicated that the original calculation of Abrahams *et al* was in error and that the value of T_1 should in fact be much smaller. The modified value is, however, still too large to agree with our data.

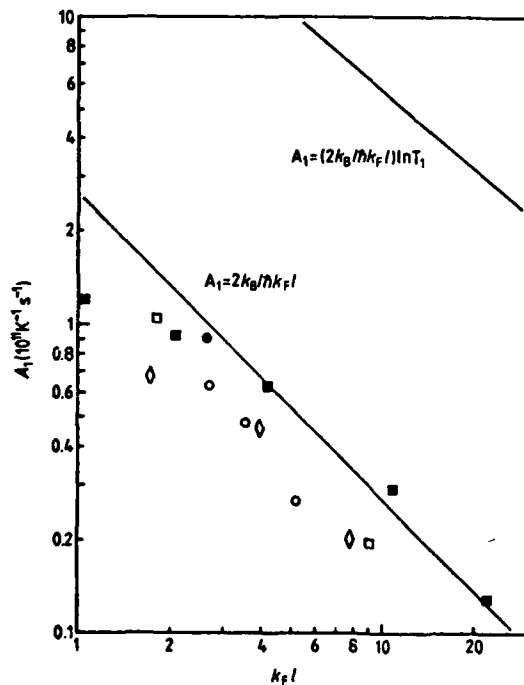


Figure 5. A_1 is plotted as a function of $k_{F1}l$ with the two proposed theoretical curves for comparison. The devices are ● CC8116/1, □ CC8116/2, ○ CC8116/3, ◇ CC8116/4 and ■ JH1/15.

Guiliani and Quinn (1982) have found a logarithmic term in the conventional result

$$\frac{1}{\tau_i} \sim \frac{(kT)^2}{\hbar E_F} \ln(E_F/kT).$$

Fukuyama (private communication) has indicated that in this presence of disorder this becomes

$$\frac{1}{\tau_i} \sim (kT)^2/\hbar E_F \ln(E_F \tau/h).$$

This is not inconsistent with the results, and might account for the scatter in figure 4.

It is a pleasure to thank Professor Sir Nevill Mott, Dr J H Davies, Professor H Fukuyama and Dr M Kaveh for many discussions on this topic. This work was supported by SERC and, in part, by the European Research Office of the US Army. R A Davies acknowledges an SERC Research Studentship.

References

- Abrahams E, Anderson P W, Lee P A and Ramakrishnan T V 1981 *Phys. Rev. B* **24** 6783
 Abrahams E, Anderson P W, Licciardello D C and Ramakrishnan T V 1979 *Phys. Rev. Lett.* **44** 1288
 Abramowitz M and Stegun I A 1970 *Handbook of Mathematical Functions* (New York: Dover)
 Altshuler B L and Aronov A G 1979 *JETP Lett.* **30** 483
 Altshuler B L, Aronov A G and Lee P A 1980a *Phys. Rev. Lett.* **44** 1288
 Altshuler B L, Khmel'nitzkii D E, Larkin A I and Lee P A 1980b *Phys. Rev. B* **22** 5142
 Ashcroft N W and Mermin N D 1976 *Solid State Physics* (New York: Holt, Rinehardt and Winston)
 Bishop D J, Dynes R C and Tsui D C 1982 *Phys. Rev. B* **26** 773
 Fukuyama H 1980a *J. Phys. Soc. Japan* **49** 649
 — 1980b *J. Phys. Soc. Japan* **49** 2169
 — 1981 *J. Phys. Soc. Japan* **50** 3407
 — 1982 *Surface Sci.* **113** 489
 Gorkov L P, Larkin A I and Khmel'nitzkii D E 1979 *JETP Lett.* **30** 248
 Guiliani G F and Quinn J J 1982 *Phys. Rev. B* **26** 4421
 Hikami S, Larkin A I and Nagaoka Y 1980 *Prog. Theor. Phys.* **63** 707
 Kaveh M and Mott N F 1981 *J. Phys. C: Solid State Phys.* **14** L177
 Kawaguchi Y and Kawaji S 1980 *J. Phys. Soc. Japan* **49** 983
 — 1982 *Surface Sci.* **113** 505
 Poole D A, Pepper M and Glew R J 1981 *J. Phys. C: Solid State Phys.* **14** L995
 Poole D A, Pepper M and Hughes A 1982 *J. Phys. C: Solid State Phys.* **15** L1137
 Schmid A 1974 *Z. Phys.* **271** 251
 Stern F 1980 *Phys. Rev. Lett.* **44** 1469
 Uren M J, Davies R A, Kaveh M and Pepper M 1981a *J. Phys. C: Solid State Phys.* **14** L395
 — 1981b *J. Phys. C: Solid State Phys.* **14** 5935
 Wheeler R G 1981 *Phys. Rev. B* **24** 4645

END

FILMED

10-84

DTIC